THE DESIGN, FABRICATION AND TESTING OF PASSIVE MICROSTRIP CIRCUITS

by

WILLIAM ALLEN ROSENKRANZ

B.S.E.E., Kansas State University, 1967
B.S., Math., Kansas State University, 1968

A MASTER'S REPORT

submitted in partial fulfillment of the

requirements for the degree

MASTER OF SCIENCE

Department of Electrical Engineering

KANSAS STATE UNIVERSITY
Manhattan, Kansas

1972

Approved by:

Dale E. Kaufman
Major Professor

PREFACE

The objective of this report is to assimilate from the published literature and place in one report the pertinent information necessary to design a microstrip transmission line. This report does not contain an analysis of the microstrip line; for such an analysis see references (1, 2).

A thick film procedure was used to fabricate microstrip lines for testing. The choice of this method of fabrication does not imply that this method is superior to other methods. Rather, this method was chosen since the necessary materials and equipment were readily available in the Department of Electrical Engineering.

A passive device, in this case a directional coupler, was selected as a design test device so as to incorporate a microstrip transmission line.

Finally, the microwave microstrip transmission lines and directional couplers that were fabricated were tested and an account of the results is given.

TABLE OF CONTENTS

Chapter		Page
I.	MICROSTRIP TRANSMISSION LINE CHARACTERISTICS . .	1
	1.0 Introduction	1
	1.1 Characteristic Impedance	2
	1.2 Microstrip Line Effective Wavelength . . .	7
	1.3 Effective Dielectric Constant and Filling Fraction	7
	1.4 Microstrip Losses	10
II.	DESIGN AND FABRICATION OF MICROSTRIP TRANSMISSION LINES	12
	2.1 Design of Microstrip Transmission Lines .	12
	2.2 A Microstrip Design	13
	2.3 Microstrip Bends	14
	2.4 Coupling to Microstrip Transmission Lines	14
	2.5 Fabrication of Microstrip Circuits	16
III.	DESIGN AND FABRICATION OF MICROSTRIP DIRECTIONAL COUPLERS	18
	3.0 Introduction to Directional Couplers . . .	18
	3.1 Classification of Directional Couplers . .	18
	3.2 Scattering Matrix Analysis of a Directional Coupler	19
	3.3 Normal Mode Analysis of a Directional Coupler	25

Chapter Page

3.4 A Microstrip Directional Coupler Design Procedure 31

IV. TESTING OF MICROSTRIP TRANSMISSION LINES AND DIRECTIONAL COUPLERS 35

4.1 Design Specifications 35

4.2 Microstrip Transmission Line Data 36

4.3 Microstrip Directional Couplers Data . . . 40

4.4 Summary 54

ACKNOWLEDGMENTS 58

REFERENCES 59

FIGURES 60

APPENDIX 78

LIST OF FIGURES

Figure		Page
1.	Various Microwave Transmission Lines (Longitudinal View)	60
2.	Detailed Microstrip Line	60
3.	Wheeler's Original Parallel Plane Waveguide	61
4.	Mapping of the Indicated Quadrant of Fig. 8	61
5.	Characteristic Impedance of Microstrip Lines-- Wide Strip Approximation ($w/h > 1.0$)	62
6.	Characteristic Impedance of Microstrip Line-- Narrow Strip Approximation ($w/h < 1.0$)	63
7.	Enclosed Microstrip	64
8.	Characteristic Impedance of Enclosed and Open Microstrip Lines	64
9.	Ratio of Free Space Wavelength (λ_o) to Microstrip Wavelength (λ_m)	65
10.	Microstrip Effective Dielectric Constant	67
11.	Microstrip Filling Fraction	67
12.	Microstrip Bends	68
13.	Microstrip Directional Coupler and Test Fixture	69
14.	Scattering Parameters Associated with a Directional Coupler	71
15.	Even and Odd Mode Representation	72
16.	Cascade Matrix Circuit Representation	73
17.	Transmission Line Representation	73
18.	Microstrip Directional Coupler	74

Figure Page

19. Design Curves for Microstrip Directional Coupler (ϵ_r = 8.9) 75

20. VSWR Insertion Loss Versus Frequency; Straight Microstrip Line (w/h = 1.0) 76

A1. Exposure of Screen Mask 77

A2. Mask to Screen Transfer 77

LIST OF TABLES

Table		Page
I.	Test Data on Straight Microstrip Lines	37
IIA.	Microstrip with Gradual Bends	38
IIB.	Microstrip with Right Angle Bends	38
IIC.	Microstrip with 45-degree Bends	39
IIIA.	Microstrip Directional Coupler Test Data (Port 1 is input port)	41
IIIB.	Microstrip Directional Coupler Test Data (Port 2 is input port)	44
IIIC.	Microstrip Directional Coupler Test Data (Port 3 is input port)	47
IIID.	Microstrip Directional Coupler Test Data (Port 4 is input port)	50

CHAPTER I

MICROSTRIP TRANSMISSION LINE CHARACTERISTICS

1.0. Introduction

The microstrip transmission line is one of several transmission lines available to the microwave engineer (Fig. 1). The development of miniaturized microwave devices, solid-state microwave electronics, hybrid microwave assemblies, and microwave integrated circuits has led to the need for a compatible transmission system, namely, the microstrip line. This type of transmission line permits the interconnection of miniaturized passive and active devices within a single package and reduces the need for connectors with their associated interfacing problems. The advances in dielectric material technology, as well as the need for increased miniaturization and improved compatibility, have thus revived interest in the microstrip transmission line.

The basic geometry of the microstrip line is shown in Fig. 2. The microstrip line is an open transmission line in comparison to the strip line, coaxial and waveguide transmission lines. That is, coaxial lines and waveguides have a conductor completely surrounding the transmission line, while the strip line has a center conductor width small enough in contrast to the width of the two ground planes that it can be considered a closed line. In comparison, the microstrip line has a conductor only on one side of the center conductor. Also it should be

noted that the microstrip line has a nonuniform dielectric surrounding its center conductor, whereas the other three transmission lines make use of a uniform dielectric.

It is this difference in the geometry and dielectric structure of the microstrip line, as compared with the other three types of transmission lines, that makes the analysis of the microstrip line more difficult.

In the microstrip line there is a dielectric, usually air, above and on both sides of the center conductor as well as a dielectric material having a relative permittivity ϵ_r between the center conductor and the ground plane. The range of values of ϵ_r, for different dielectric substrates used with microstrip lines, has been as low as 2.32 and as high as 100.[3, 4] It is the application of the particular microstrip device that dictates the particular dielectric substrate types that can be used.

Of principal interest in characterizing a microstrip line are the line's characteristic impedance, losses, and effective electrical length. Each of these three parameters will subsequently be discussed. Being able to predict adequately the characteristic impedance (Z_o) of a microstrip line and then to fabricate a line having the required characteristic impedance is the first concern for a microwave engineer using microstrip.

1.1. Characteristic Impedance

The characteristic impedance of microstrip lines can be obtained from the analysis by H. A. Wheeler.[1, 2] The characteristic impedance predicted by Wheeler's graphs and formulas have been verified experimentally in this report and by

others.[2,3,4,6,7] In the interest of brevity, only the appropriate results of Wheeler's work will be given here.

Wheeler's work was based on a conformal mapping analysis of a parallel plane waveguide (Figs. 3, 4). A brief discussion of the conformal mapping analysis is given in section 1.3. This work assumes transverse electromagnetic (TEM) propagation and includes the effects of the dielectric discontinuity. From this work a set of reliable microstrip design curves is available.[2] This set of microstrip characteristic impedance curves is shown in Figs. 5 and 6. Note that in Fig. 5 the range of the abscissa values (w/h) is from 0.50 to 40 and in Fig. 6 from 0.01 to 1.0.

Wheeler's treatment of the microstrip problem was divided into two cases according to the a/b ratio of the waveguide (Fig. 3). These two cases were wide strips ($a/b > .3$) and narrow strips ($a/b < .3$). Correspondingly, Wheeler has given two equations, one for the narrow strip and one for wide strip conditions, these equations applying directly to the parallel plane waveguide. These equations give the characteristic impedance (Z_o) and shape (a/b) explicitly in terms of the parallel plane guide geometry and the supporting dielectric relative permittivity. A transformation must be made on these equations so that they apply to the microstrip line. This transformation is based on the following considerations:

(a) $w = 2a$, $h = b$ (Figs. 2, 3)

(b) $2\ Z_{o\ \text{microstrip}} = Z_{o\ \text{parallel plane}}$.

For a given dielectric with a relative permittivity (ϵ_r) and a desired characteristic impedance (Z_o), the shape ratio

(w/h) for the microstrip line is given as:

Narrow lines ($w/h \leq 1.0$)

$$\frac{w}{h} = \frac{4}{1/2\ e^{c} - e^{-c}} \tag{1.1}$$

$$c = \frac{\sqrt{\frac{\epsilon_r + 1}{2}}\ Z_o}{60} + \left(\frac{\epsilon_r - 1}{\epsilon_r + 1}\right)\left(.226 + \frac{.120}{\epsilon_r}\right)$$

Wide lines ($w/h \geq 1.0$)

$$\frac{w}{h} = .637\left\{\left(\frac{\pi\eta}{2\sqrt{\epsilon_r}\ Z_o} - 1\right) - \ln\left(\frac{\pi\eta}{\sqrt{\epsilon_r}\ Z_o} - 1\right) + \frac{\epsilon_r - 1}{2\epsilon_r}\left[\ln\left(\frac{\pi\eta}{2\sqrt{\epsilon_r}\ Z_o} - 1\right) + .293 - \frac{.517}{\epsilon_r}\right]\right\} \tag{1.2}$$

where η = free space impedance = $377\ \Omega$.

The distinction between narrow and wide lines is not absolute because there is some overlap in the definition of wide and narrow strips as formulated by Wheeler. If the (w/h) ratio is close to the value (1.0), then both relations should be used and the results compared. For values of ($w/h \leq .85$) and ($w/h \geq 1.1$) only the appropriate equation should be used. This last statement is especially valid for the case where $\epsilon_r \geq 9.0$. Also it is recommended that in the range $.85 < w/h < 1.1$, the mean value of the characteristic impedance (Z_o) as calculated from Eqs. 3 and 4 be used.

A transformation of Wheeler's equations for the parallel plane waveguide yields the following relations for the characteristic impedance of the microstrip line.

$$Z_o = \frac{120}{\sqrt{2(\epsilon_r+1)}}\left[\ln\left(\frac{8h}{w}\right) + \frac{1}{32}\left(\frac{w}{h}\right)^2 - \left(\frac{\epsilon_r-1}{\epsilon_r+1}\right)\left(.226 - \frac{.120}{\epsilon_r}\right)\right] \quad (1.3)$$

$$(w/h < 1.0)$$

$$Z_o = \frac{\eta/2\sqrt{\epsilon_r}}{\frac{w}{2h} + .441 + \left(\frac{\epsilon_r+1}{2\pi\epsilon_r}\right)\left[\ln\left(\frac{w}{2h} + .94\right) + 1.45\right] + \frac{\epsilon_r-1}{\epsilon_r^2}(0.082)} \quad (1.4)$$

$$(w/h > 1.0).$$

It has been verified that the curves given in Figs. 5 and 6 can be generated by using Eqs. 1.1, 1.2, 1.3, and 1.4.

The characteristic impedance (Z_o) curves shown in Figs. 5 and 6 were calculated for a zero thickness conductor and an infinitely wide ground plane. The center conductor, however, does have finite thickness, the principal effect of which is to increase the capacitance of the line. An approximate correction can be made for this by replacing the actual width by an effective width:[2]

$$w_{eff} = w + \Delta w \quad (1.5)$$

where

$$\Delta w = \frac{t}{\pi}\left(\ln\frac{2h}{t} + 1\right) \qquad \left(\frac{w}{2} > \frac{h}{4\pi} > t\right) \quad (1.6)$$

and

$$\Delta w = \frac{t}{\pi}\left(\ell n \frac{4\pi w}{t} + 1\right) \qquad \left(\frac{h}{4\pi} > \frac{w}{2} > t\right) \tag{1.7}$$

For precise calculation of (Z_o) this thickness correction factor should be considered. However, in Chapter II, which deals with the design and fabrication of microstrip transmission lines, it will be shown that the utilization of this thickness correction factor has little effect on the overall results.

The microstrip work discussed in this report was accomplished with an unshielded test fixture. Most industrial applications will require a metallic enclosure or packaging around the microstrip line to provide hermetic sealing and strength. The presence of such a metallic enclosure around the microstrip line changes the value of the characteristic impedance for a given w/h ratio from that of the unenclosed case. Figure 8 compares the characteristic impedance for both the enclosed (Fig. 7) and unenclosed (Fig. 2) microstrip lines[5] for a particular dielectric constant and microstrip geometry.

For a (w/h) ratio equal to or larger than unity, and with the relative permittivity equal to or greater than approximately 9,[5] the characteristic impedance of a metallically enclosed microstrip line differs little from that of an open microstrip line provided that the (ℓ/h) ratio is 3 or larger. The (ℓ/h) ratio is the ratio of the spacing (ℓ) between the center conductor and the bottom of the top wall of the metallic enclosure, and the ground plane spacing (h). With a metallic enclosure, there is a minimum spacing (s) that the edge of the center conductor can be from the metallic side wall without influencing

the fringing field (Fig. 7). From empirical strip line and microstrip work the minimum distance (s) has been determined to be of the same order of magnitude as the dimension (ℓ) in Fig. 7.

In essence, it is the center conductor width to ground plane spacing ratio (w/h) and the relative permittivity of the supporting dielectric substrate that determines the characteristic impedance of a microstrip line.

1.2. Microstrip Line Effective Wavelength

A knowledge of the effective wavelength in a microstrip transmission system is a necessity when designing directional couplers, impedance transformers, etc. Because the microstrip line is not a symmetrical transmission line, the calculation of the effective wavelength is not straightforward. The results of H. A. Wheeler's work[1, 2] have cleared the way for the determination of the effective wavelength (λ_m) in a microwave transmission line. Figure 9 shows graphically the free space wavelength to microstrip wavelength ratio (λ_o/λ_m) for various center conductor width to ground plane spacing ratios (w/h) and different dielectric relative permittivities (ϵ_r).[5]

1.3. Effective Dielectric Constant and Filling Fraction

There are two quantities, effective dielectric constant (ϵ_{eff}) and filling fraction (q), which now need to be defined and made available for calculation because of their widespread usage in the literature pertaining to microstrip and microstrip devices. Wheeler[2] has defined the filling fraction as

$$q = \frac{\text{Dielectric area containing flux lines}}{\text{Total area in the rectangle of field mapping}} .$$

The simplest way to intuitively understand what is meant by filling fraction and effective dielectric constant is to examine pictorially what Wheeler has done in his mapping procedure.[1, 2]

A portion of the parallel plane waveguide (Fig. 3) has been mapped into the Z'-plane of flux and potential coordinates (Fig. 4). This mapping reduces the problem of two finite conductors and a mixed dielectric to a problem of two infinite conductors enclosing a space containing a mixed dielectric (Fig. 4).

The dielectric substrate has a permittivity ϵ_r. The curved line between points 3 and 7 (Fig. 3) represents a free space flux line that would terminate on the edge of the conductors if the dielectric substrate were not present ($\epsilon_r = 1$). It is the presence of the dielectric sheet that complicates the analysis because of the distortion of the flux lines between the two conductors.

The dielectric region is composed of two areas. These two areas are indicated by crosshatched and horizontal lines. The crosshatched area represents the region that would contain most of the flux lines between the two conductors if the relative permittivity were unity. This area is always more than half of the total area in the rectangle of field mapping.[2] The total area in the rectangle of field mapping is the area enclosed by the points 1-2-4-6-8. The horizontally lined area represents the dielectric area (denoted by f, the fringe area) through which the distorted fringe flux lines pass. The a/b ratio (w/h for

microstrip) essentially determines the filling fraction (q) since the relative permittivity of the dielectric substrate would normally be equal to or greater than 9 in actual practice. From Wheeler[2]

$$q = \frac{\epsilon_{eff} - 1}{\epsilon_r - 1}, \qquad 0 < q < 1 \qquad (1.8)$$

$$\epsilon_{eff} \geq 1 .$$

If the center conductor of the microstrip line were widened, say to the width of the ground plane as in a parallel plate waveguide, then q would approach unity and ϵ_{eff} would approach the relative permittivity (ϵ_r) of the substrate. For this condition all the flux lines would essentially be contained between the conducting plates. If the center conductor width were decreased to almost zero, the filling fraction (q) would approach a value of 0.5.

In essence, the filling factor and effective permittivity indicate the ratio of flux lines passing from the bottom portion of the center conductor to the ground plane as compared to the flux lines passing from the top portion of the center conductor to the ground plane.

From the work of Wheeler[1, 2] and Seckelmann,[7] Figs. 10 and 11 give curves for calculating the filling fraction and effective permittivity. The filling fraction can be found from Fig. 11 and is essentially a function of only the (w/h) ratio.

1.4. Microstrip Losses

The loss per unit length of a microstrip transmission line will be approximated using the parallel plane guide as a model. The total loss (α) will be considered as a summation of the losses in the two conductors (α_c) and the supporting dielectric substrate (α_d).

$$\alpha = \alpha_c + \alpha_d \tag{1.9}$$

If the spacing between the center conductor and the ground plane is less than one-half wavelength, then substantially all the energy is in the TEM mode and the operating frequency is below the cutoff frequency for higher order modes.

Assuming that the two conducting planes represent good conductors and that the only mode that is propagating is the TEM mode, then the conductor loss can be represented by

$$\alpha_c = \frac{\sqrt{\pi f \mu_m}}{2 Z_o w} \left(\frac{1}{\sqrt{\sigma_{c1}}} + \frac{1}{\sqrt{\sigma_{c2}}} \right) \quad \text{nepers/meter} \tag{1.10}$$

where σ_{c1}, σ_{c2} represent the conductivity of the two conducting plates

μ_m is permeability of the conducting plates (presumably the same for both plates)

w is the respective width of the plates, assumed here to be equal.

The dielectric loss for the microstrip line modeled by the parallel plane guide and assuming a good dielectric, is given by

$$\alpha_d = \frac{\omega}{2}\sqrt{\frac{\mu_d}{\epsilon_r'}}\left(\frac{\epsilon_r''}{\epsilon_r'}\right)\epsilon_r' = \frac{gZ_o}{2} \quad \text{nepers/meter} \tag{1.11}$$

where

$\epsilon_r = \epsilon_r' - j\epsilon_r''$, complex dielectric constant

Z_o = characteristic impedance of microstrip line

g = the conductivity of the dielectric

μ_d = relative permeability of the dielectric.

The total loss is approximated as

$$\alpha = \frac{1}{8.68}\left(\frac{\sqrt{\pi f \mu_m}}{Z_o w \sqrt{\sigma_c}} + \frac{gZ_o}{2}\right) \quad \text{db/meter} \tag{1.12}$$

where

$\sigma_{c1} = \sigma_{c2} = \sigma_c$, since both conductors are of the same material.

A typical range of values for α is $12 < \alpha < 20$ db/meter.

CHAPTER II

DESIGN AND FABRICATION OF MICROSTRIP TRANSMISSION LINES

2.1. Design of Microstrip Transmission Lines

The design of a microstrip transmission line will depend upon the application, which in turn dictates the type and dimensions of the supporting dielectric substrate. In particular, the relative permittivity, loss tangent, and surface finish of the substrate will be the major factors in selecting a substrate material.

The length and width of the substrate will be determined by the type and number of both passive and active devices that are to be mounted on a single substrate. Typically, one- and two-inch squares are readily available commercially. Other sizes are available upon special order. However, the time lag in receiving such special orders, because of the new tooling required and the greatly increased cost of obtaining especially shaped substrates, limits small scale prototype microstrip work to standard size substrates. The thickness of "off the shelf" commercially available substrates is also determined by the manufacturer.

The substrates used in conjunction with this report were one inch square and .025 inch thick. The relative permittivity was 8.9. The substrates, Alumina AD-96, were manufactured by the Coors Porcelain Company.

2.2. A Microstrip Design

With the substrate thickness (h = .025 inch) and relative permittivity (ϵ_r = 8.9) determined, the selection of the desired characteristic impedance for the microstrip line will determine the width (w) of the center conductor. A characteristic impedance of 50 ohms was selected and from Fig. 5 a (w/h) ratio of 1 was determined.

A thick film process was used to form the center conductor and ground plane. Unfortunately, the thickness of the center conductor was not constant along the line of each substrate and varied from substrate to substrate. Of more than 30 thickness measurements that were made on three substrates, the following variation in center conductor thickness was observed:

$$t_{max} = .00094 \text{ inch}$$
$$t_{min} = .00057 \text{ inch}$$
$$t_{ave} = .00071 \text{ inch.}$$

Using $t = t_{ave}$, the width correction factor (Δw) (Eq. 1.7) was calculated to be approximately 10^{-3} inch. Considering the observed tolerance on the width of the center conductor, i.e., w = .025 $\pm$.001 inch, the effective width correction factor was not incorporated in this design. However, with a more refined thick film procedure (or with a refined thin film procedure), where a strip width tolerance of .5 mil or better could be maintained, the strip width correction factor should be employed. With a $\pm$.001-inch width variation around the desired .025-inch width, the VSWR of the line would be less than 1.03, providing

other impedance mismatches do not occur along the line or at the connections to the line.

2.3. Microstrip Bends

In any microwave system bends in the transmission line will occur because of physical layout design constraints. Being able to design bends in microstrip lines is a necessity since system requirements may require that the transmission lines emanating from a device mounted on a dielectric substrate may not follow straight lines. Because of the nature of the symmetry between strip transmission line and microstrip transmission line, the type of bends used in strip transmission lines have been applied to microstrip transmission lines. Three types of bends to accomplish a 90-degree bend have been developed and are shown in Fig. 12. However, 90-degree bends are not always required and an appropriate modification of these bends may be necessary.

2.4. Coupling to Microstrip Transmission Lines

After the center conductor and ground plane have been deposited on the dielectric substrate, some means of connecting to the center conductor is needed. This connection must also be matched to the characteristic impedance of the microstrip line. Usually, standard microwave connectors are designed for 50-ohm characteristic impedance. If the particular microwave device on the substrate does not have a 50-ohm input impedance, then the microstrip transmission line must perform the necessary impedance transformation between the device and the connector.

In Fig. 13 an Omni-Spectra substrate holder and four connectors are shown. This substrate holder and connectors comprised the test fixture used to mount the substrate and to provide the interface between the microstrip line and peripheral test equipment. The substrate holder is necessary not only for the mounting of the connectors but also to give mechanical support to the dielectric substrate.

The connector uses a center tab which can be either butt-jointed or overlapped with the microstrip center conductor. It is desirable that the width of the center conductor tab be the same as the center conductor strip width. If the connector is to be permanently attached to the substrate, then the center tab of the connector should be tapered to match the microstrip conductor width before it is soldered to the microstrip center conductor. The soldering operation will keep the center tap centered with respect to the microstrip center conductor.

If there is a limitation on the number of connectors and substrate holders available, or if only one test fixture is to be used in conjunction with the testing of many microstrip devices, then the center tab of the connector should not be extensively altered nor soldered because of its fragile construction.

On the peripheral side of the connector is an OSM connector to which an OSM to type N adaptor was placed to complete the connector transition.

2.5. Fabrication of Microstrip Circuits

Two basic methods of fabricating microstrip circuits have received general interest. These two methods involve thick film and thin film techniques. Two other methods, seldom used, are fabrication by electroplating the conductor material on a substrate or etching the desired conductor pattern from one side of a di-clad copper-covered teflon board.

Principally, thick film techniques were used to fabricate the microstrip lines investigated in this report.

The materials used in the thick film procedure were:

(a) Dielectric substrate--Coors ceramic AD-96

(b) Conductor paste--Silver palladium.

The dielectric substrate characteristics were:

Dielectric constant (relative)* $\epsilon_r = 8.9$

Loss tangent* $\tan \delta = 0.0001$

Surface finish (ground typical) ave. 50 μ in.

Resistivity* $>10^{14}$ ohm-cm.

Because the average thickness of both the center conductor and ground plane was more than 10 times the nominal figure given for the surface finish, there was no problem encountered in forming a continuous uninterrupted center conductor, even though the surface of these substrates was 'rough'. In contrast, center conductors deposited on such a surface using thin film techniques would not be satisfactory, for whenever the center conductor is thin a noncontinuous line is highly probable after

---

*Measured at 25 degrees C. and 1 GH_z.

the etching process has been completed, i.e., the etchant has etched through the line forming a discontinuity.

Once the conductor width, dielectric substrate, and conductor material have been selected, the fabrication process basically follows the following format.

(a) Art work: Construct a pattern that is scaled N:1 with respect to the desired end product, $N > 1$.

(b) Photography: Photograph the art work and reduce it to desired size.

(c) Mask and screen preparation: Use the developed negative to develop a light sensitive mask and transfer the mask to a screen.

(d) Printing: Use the screen with its imprinted mask to form a pattern on the substrate; a squeegee is moved across this screen to deposit the conductor paste on the substrate.

(e) Firing the substrate: After depositing the conductor paste, fire the substrate in an appropriate oven.

Explicit details of the thick film procedure are given in the Appendix. Upon completion of these steps the microstrip device is ready for testing.

The devices fabricated and tested here have been a result of the thick film procedure. A thin film procedure was tried but the etching process required negated any results.

CHAPTER III

DESIGN AND FABRICATION OF MICROSTRIP DIRECTIONAL COUPLERS

3.0. Introduction to Directional Couplers

Chapters I and II provide guide lines for the use and design of a microwave microstrip transmission line. A directional coupler was selected as the passive device in order to illustrate the use of a microstrip line. Section 3.1 will discuss the classification of directional couplers. Then in sections 3.2 and 3.3 a scattering matrix and normal mode analysis of a microstrip directional coupler is given; such an analysis demonstrates certain general properties common to directional couplers. From this the desired coupler electrical length, the input-output characteristics of an ideal coupler, and the voltage coupling coefficient are given. In section 3.4, the necessary design information for a microstrip directional coupler is given. This includes strip width and spacing for the coupler.

3.1. Classification of Directional Couplers

Directional couplers may be classified in a number of ways.[9] Only the classification categories that apply to a microstrip directional coupler will be considered; they are:

(a) Classification by the type of transmission system (waveguides, coaxial lines, strip line, microstrip line, quasi-optical guides, etc.).

(b) Classification as codirectional or contradirectional directional couplers. In a codirectional coupler the coupled wave travels in the same direction as that of the wave in the main line, while in the contradirectional coupler the coupled wave travels in the opposite direction.

(c) Classification by the form of coupling. Since coupling depends largely upon the transmission line, there are many ways of achieving coupling. Some of the methods are: single aperture and multiple aperture coupling, continuous (longitudinal) aperture coupling, waveguide junctions, ring couplers, etc.

The type of directional coupler most applicable to a microstrip system is a microstrip-TEM coupler, codirectional or contradirectional coupler, depending on the final design, with continuous (longitudinal) aperture coupling.

3.2. Scattering Matrix Analysis of a Directional Coupler

Two basic analysis approaches to directional couplers will be considered and then design curves and equations will be given in order to formulate a design procedure.

The first approach (as does the second) gives information on the general properties of a directional coupler. This approach utilizes the properties of a scattering matrix to characterize from an external point of view the directional coupler as a "black box". Consider a 4-port directional coupler as shown in Fig. 14. The incident waves are denoted by a_1, a_2,

a_3, a_4, and the reflected waves by b_1, b_2, b_3, b_4. Thus this 4-port directional coupler can be considered as a 4-port network where the a_i (i = 1, 2, 3, 4) represent the incident voltage waves and the b_i (i = 1, 2, 3, 4) represent the reflected voltage waves. Since this coupler is a linear four-terminal device it can be represented by four linear equations.

$$b_1 = s_{11}a_1 + s_{12}a_2 + s_{13}a_3 + s_{14}a_4$$

$$b_2 = s_{21}a_1 + s_{22}a_2 + s_{23}a_3 + s_{24}a_4$$

$$b_3 = s_{31}a_1 + s_{32}a_2 + s_{33}a_3 + s_{34}a_4$$

$$b_4 = s_{41}a_1 + s_{42}a_2 + s_{43}a_3 + s_{44}a_4 \,, \tag{3.1}$$

which can be expressed in matrix form

$$b_i = \sum_{i,j=1}^{N} s_{ij}\, a_j \tag{3.2}$$

or

$$\left[B\right] = \left[S\right]\left[A\right]$$

where

b_i are the elements of the column vector $\left[B\right]$ representing the scattered waves at the four ports,

a_j are the elements of the column vector $\left[A\right]$ representing the input waves at the four ports,

s_{ij} are the scattering matrix elements of the network, and $\left[S\right]$ is a 4x4 matrix.

The scattering matrix is interpreted as follows:

(a) The nondiagonal elements ($i \neq j$) represent the transmission coefficients between ports i and j,

(b) The diagonal elements ($i = j$) represent the reflection coefficients of the i^{th} port.

A directional coupler is a passive, reciprocal, linear four-port device. Since the network is reciprocal the scattering matrix will have the following properties:

(a) Because of reciprocity

$$[S] = [S]^T .$$

Furthermore,

(b) if the network is lossless, the scattering matrix is unitary,

$$[S] = [S]^T = [S^*]^{-1}$$

where $[S^T]$ is the transpose of $[S]$

and $[S^*]^{-1}$ is the complex conjugate inverse of $[S]$.

Figure 14 represents one model of the coupler fabricated in conjunction with this report. The coupler is assumed to be symmetric with a slight mismatch occurring at all four ports so that there is only finite isolation between the input and isolated port. Also it is assumed that the slight mismatch does not disturb the symmetry of the coupler.

The elements of the scattering matrix take the form

$$s_{11} = s_{22} = s_{33} = s_{44}$$

$$S_{12} = S_{21} = S_{34} = S_{43} \tag{3.3}$$

$$S_{13} = S_{31} = S_{24} = S_{42}$$

$$S_{14} = S_{41} = S_{23} = S_{32}$$

and the scattering matrix becomes

$$[S] = \begin{bmatrix} S_{11} & S_{12} & S_{13} & S_{14} \\ S_{12} & S_{11} & S_{14} & S_{13} \\ S_{13} & S_{14} & S_{11} & S_{12} \\ S_{14} & S_{13} & S_{12} & S_{11} \end{bmatrix} \tag{3.4}$$

From the property,

$$[S]\,[S^*] = [I] \tag{3.5}$$

where $[I]$ is the identity matrix.

The following equations (3.6) are generated.

$$\begin{aligned} &\text{(a)} \quad S_{11}S_{11}^* + S_{12}S_{12}^* + S_{13}S_{13}^* + S_{14}S_{14}^* = 1 \\ &\text{(b)} \quad S_{11}S_{12}^* + S_{12}S_{11}^* + S_{13}S_{14}^* + S_{14}S_{13}^* = 0 \\ &\text{(c)} \quad S_{11}S_{13}^* + S_{12}S_{14}^* + S_{13}S_{11}^* + S_{14}S_{12}^* = 0 \\ &\text{(d)} \quad S_{11}S_{14}^* + S_{12}S_{13}^* + S_{13}S_{12}^* + S_{14}S_{11}^* = 0 \,. \end{aligned} \tag{3.6}$$

Thus it follows that

$$s_{11}s_{13}^* + s_{12}s_{14}^* = -(s_{13}s_{11}^* + s_{14}s_{12}^*)$$
$$s_{11}s_{14}^* + s_{12}s_{13}^* = -(s_{13}s_{12}^* + s_{14}s_{11}^*) \qquad (3.7)$$

and

$$(s_{11}s_{13}^* + s_{12}s_{14}^*)(s_{13}s_{12}^* + s_{14}s_{11}^*)$$
$$= (s_{11}s_{14}^* + s_{12}s_{13}^*)(s_{13}s_{11}^* + s_{14}s_{12}^*) \qquad (3.8)$$

so that

$$(|s_{11}|^2 - |s_{12}|^2)(s_{13}^*s_{14} - s_{13}s_{14}^*)$$
$$= (|s_{13}|^2 - |s_{14}|^2)(s_{11}^*s_{12} - s_{11}s_{12}^*). \qquad (3.9)$$

For the present assume that perfect isolation exists between ports 1 and 2, i.e., $s_{12} = 0$. Then Eqs. (3.6) and (3.9) reduce to

$$\begin{aligned}
&\text{(a)} \quad |s_{11}|^2 + |s_{13}|^2 + |s_{14}|^2 = 1 \\
&\text{(b)} \quad s_{13}s_{14}^* + s_{14}s_{13}^* = 0 \\
&\text{(c)} \quad s_{11}s_{13}^* + s_{13}s_{11}^* = 0 \\
&\text{(d)} \quad s_{11}s_{14}^* + s_{14}s_{11}^* = 0 \\
&\text{(e)} \quad |s_{11}|^2 (s_{13}^*s_{14} - s_{13}s_{14}^*) = 0 \ .
\end{aligned} \qquad (3.10)$$

These equations have a unique solution if $s_{11} = 0$ or if both s_{13} and $s_{14} = 0$. For s_{13} and s_{14} equal to zero there is no response at the output ports (ports 3 and 4); this is a degenerate case of no interest. Hence for perfect isolation $s_{11} = 0$; thus the input port must be perfectly matched. For

$s_{11} = 0$, Eqs. (3.10) reduce to

$$\begin{aligned} &(a) \quad |s_{13}|^2 + |s_{14}|^2 = 1 \\ &(b) \quad s_{13}s_{14}^* + s_{14}s_{13}^* = 0 \ . \end{aligned} \tag{3.11}$$

Then

$$s_{13} = |s_{13}|e^{j\theta_3} \ , \quad s_{14} = |s_{14}|e^{j\theta_4} \ . \tag{3.12}$$

Then Eq. (3.11b) can be rewritten as

$$0 = |s_{13}|e^{j\theta_3}\,|s_{14}|e^{-j\theta_4} + |s_{14}|e^{j\theta_4}\,|s_{13}|e^{-j\theta_3} \tag{3.13}$$

or

$$|s_{13}||s_{14}|(e^{j(\theta_3-\theta_4)} + e^{j(\theta_4-\theta_3)}) = 0 \tag{3.14}$$

and finally

$$\cos(\theta_3 - \theta_4) = 0 \ . \tag{3.15}$$

Since

$$|s_{13}||s_{14}| \neq 0 \ ,$$

there is a 90-degree phase difference between the waves in the two output arms for a symmetrical coupler that is matched and has perfect isolation between the input and the isolated output arm. The scattering matrix approach to the directional coupler does not provide a complete set of design equations but does bring out certain properties for the ideal case.

3.3. Normal Mode Analysis of a Directional Coupler

A second approach to examining directional couplers is an analysis using even and odd modes. In Fig. 15, suppose the directional coupler has a plane of symmetry. The first mode of excitation considered is the even mode. Here two in-phase signals of amplitude +1/2 are applied to ports 1 and 2. Since the two signals are in phase along the plane of symmetry, there is a voltage maximum along this plane. On the symmetry plane the impedance is infinite and thus a magnetic wall (H = 0) is formed along the plane.

If two out-of-phase signals of amplitude 1/2 are applied at ports 1 and 2, a voltage minimum occurs along the plane of symmetry. Thus an electric wall (or an equivalent short circuit) is formed along the plane of symmetry.

By superposition of the even and odd modes (since this is a linear model), the normal mode field distribution corresponds to that given by a signal of unit amplitude at port 1. The resultant signals out of each port are also given by the superposition of those output signals obtained by the even and odd modes.

The reflection and transmission coefficients for the even (Γ_{oe}, T_{oe}) and odd (Γ_{oo}, T_{oo}) modes are defined as follows:

$$\text{(a)}\quad \Gamma_{oe} = b_{1e}/a_{1e} = b_{2e}/a_{2e},\quad T_{oe} = b_{3e}/a_{2e} = b_{4e}/a_{1e}$$
$$\text{(b)}\quad \Gamma_{oo} = b_{1o}/a_{1o} = b_{2o}/a_{2o},\quad T_{oo} = b_{3o}/a_{2o} = b_{4o}/a_{1o} \qquad (3.16)$$

where the (o, e) second subscript on the (a) and (b) voltage

waves denote even and odd modes and the first subscript the particular port. Thus by superposition

$$\begin{aligned}
&\text{(a)} \quad b_1 = b_{1e} + b_{1o} = 1/2(\Gamma_{oe} + \Gamma_{oo}) \\
&\text{(b)} \quad b_2 = b_{2e} + b_{2o} = 1/2(\Gamma_{oe} - \Gamma_{oo}) \\
&\text{(c)} \quad b_3 = b_{3e} + b_{3o} = 1/2(T_{oe} - T_{oo}) \\
&\text{(d)} \quad b_4 = b_{4e} + b_{4o} = 1/2(T_{oe} + T_{oo}) \ .
\end{aligned} \tag{3.17}$$

The cascade or (A-B-C-D) matrix for a transmission line is defined as follows in Eq. (3.18) and Fig. 16.

$$\begin{bmatrix} V_1 \\ I_1 \end{bmatrix} = \begin{bmatrix} A & B \\ C & D \end{bmatrix} \begin{bmatrix} V_2 \\ I_2 \end{bmatrix} \ . \tag{3.18}$$

Also, from Fig. 17, the following basic equations hold:

$$\begin{aligned}
&\text{(a)} \quad \Gamma = \frac{Z_R - Z_o}{Z_R + Z_o} \ , \quad Z_R = \frac{V_2}{I_2} \\
&\text{(b)} \quad Z_{in} = \frac{V_1}{I_1} = Z_o \left(\frac{1 + \Gamma}{1 - \Gamma}\right) \ .
\end{aligned} \tag{3.19}$$

Combining Eqs. (3.18) and (3.19), we have the reflection coefficient when $Z_R = Z_o$, or

$$\Gamma = \frac{A + B/Z_o - CZ_o - D}{A + B/Z_o + CZ_o + D} \ . \tag{3.20}$$

This solution for Γ (as well as for T and Z_{in}) is permissible

since for each normal mode the problem reduces to that of a linear two-port network.

The transmission coefficient for the cascade matrix is (9),

$$T = \frac{2}{A + B/Z_o + CZ_o + D} \tag{3.21}$$

and the input impedance is

$$Z_{in} = \frac{A + B/Z_o}{C + D/Z_o} \, . \tag{3.22}$$

For a general transmission line, the following equation (Fig. 17) holds:

$$\text{(a)} \quad Z_{in} = \frac{V_1}{I_1} = \frac{V_R \cosh \gamma\ell + Z_o I_R \sinh \gamma\ell}{I_R \cosh \gamma\ell + (V_R/Z_o) \sinh \gamma\ell}$$

$$\text{(b)} \quad \gamma = \alpha + j\beta \tag{3.23}$$

where γ is the propagation constant, α the attenuation constant, and β the phase constant. If $\alpha = 0$, i.e., the line is lossless, then

$$Z_{in} = \frac{Z_R \cos \beta\ell + Z_o \, j \sin \beta\ell}{\cos \beta\ell + \dfrac{Z_R}{Z_o} \, j \sin \beta\ell} \, . \tag{3.24}$$

If we let $\theta = \beta\ell$, the cascade matrix equation from port 1 to port 4 for the lossless directional coupler is

$$\begin{bmatrix} V_1 \\ I_1 \end{bmatrix} = \begin{bmatrix} \cos\theta & jZ_o \sin\theta \\ \dfrac{j \sin\theta}{Z_o} & \cos\theta \end{bmatrix} \begin{bmatrix} V_4 \\ I_4 \end{bmatrix} \tag{3.25}$$

where

$$A = \cos\theta \qquad B = j Z_o \sin\theta$$

$$C = \frac{j \sin\theta}{Z_o} \qquad D = \cos\theta$$

from Eq. (3.18).

Equation (3.25) can be expressed in terms of the even and odd modes, i.e., in terms of

$$V_{1e},\ V_{1o},\ I_{1e},\ I_{1o},\ \theta_e,\ \theta_o,\ V_{4e},\ V_{4o},\ Z_{oe},\ Z_{oo}$$

where θ_o and θ_e are the electrical lengths of the line for the even and odd modes, respectively.

From the expression for Γ, (Eq. 3.20),

$$\text{(a)}\quad \Gamma_{oe} = \frac{j\left[\dfrac{Z_{oe}}{Z_o} - \dfrac{Z_o}{Z_{oe}}\right] \sin\theta_e}{2\cos\theta_e + j\left[\dfrac{Z_{oe}}{Z_o} + \dfrac{Z_o}{Z_{oe}}\right] \sin\theta_e} \tag{3.26}$$

$$\text{(b)}\quad \Gamma_{oo} = \frac{j\left[\dfrac{Z_{oo}}{Z_o} - \dfrac{Z_o}{Z_{oo}}\right] \sin\theta_o}{2\cos\theta_o + j\left[\dfrac{Z_{oo}}{Z_o} + \dfrac{Z_o}{Z_{oo}}\right] \sin\theta_o} .$$

For the conditions that

$$\text{(a)}\quad \theta_o = \theta_e = \theta$$

$$\text{and}\qquad \text{(b)}\quad Z_o = (Z_{oe}Z_{oo})^{1/2} \tag{3.27}$$

it follows that

$$\text{(a)}\quad \Gamma_{oe} = -\Gamma_{oo}$$

$$\text{(b)}\quad \Gamma_{oe} = \frac{j\left[(Z_{oe}/Z_{oo})^{1/2} - (Z_{oo}/Z_{oe})^{1/2}\right]\sin\theta}{2\cos\theta + j\left[(Z_{oe}/Z_{oo})^{1/2} + (Z_{oo}/Z_{oe})^{1/2}\right]\sin\theta}. \tag{3.28}$$

From Eqs. (3.21) and (3.25) and the condition that $\theta_o = \theta_e = 0$, the transmission coefficient can be expressed as

$$T_{oe} = T_{oo} = \frac{2}{2\cos\theta + j\left[(Z_{oe}/Z_{oo})^{1/2} + (Z_{oo}/Z_{oe})^{1/2}\right]\sin\theta}. \tag{3.29}$$

From Eq. (3.17), the signals emerging from the four ports are

$$\text{(a)}\quad b_1 = 0$$

$$\text{(b)}\quad b_2 = \frac{j\left[(Z_{oe}/Z_{oo})^{1/2} - (Z_{oo}/Z_{oe})^{1/2}\right]\sin\theta}{2\cos\theta + j\left[(Z_{oe}/Z_{oo})^{1/2} + (Z_{oo}/Z_{oe})^{1/2}\right]\sin\theta} \tag{3.30}$$

$$\text{(c)}\quad b_3 = 0$$

$$\text{(d)}\quad b_4 = T_{oe} = \frac{2}{2\cos\theta + j\left[(Z_{oe}/Z_{oo})^{1/2} + (Z_{oo}/Z_{oe})^{1/2}\right]\sin\theta}.$$

By inspection of Eq. (3.30), it can be seen that the coupling to port 2 (b_2) is a maximum if the length of coupled line is a quarter wavelength ($\ell = \lambda/4$) and a minimum of zero for the line length equal to one-half a wavelength ($\ell = \lambda/2$). Also,

given a perfect match at the input port ($b_1 = 0$) and perfect isolation ($b_3 = 0$), for maximum coupling to port 2 (b_2 is a maximum) the direct output (b_4) is a minimum. Lastly, for (b_2) a minimum, the direct output (b_4) is a maximum.

The scattered wave (b_2) gives the voltage coupling (K) between the input port (1) and the coupled port (2).

For $K = b_2$, $\ell = \lambda/4$, then

$$K = \frac{\frac{Z_{oe}}{Z_{oo}} - 1}{\frac{Z_{oe}}{Z_{oo}} + 1} . \qquad (3.31)$$

The insertion loss between the input port and the output port for the ideal contradirectional coupler is

$$\frac{P_{in}}{P_{out}} = 1 + \frac{1}{4}\left[(Z_{oe}/Z_{oo})^{1/2} - (Z_{oo}/Z_{oe})^{1/2}\right]^2 \sin^2 \theta . \qquad (3.32)$$

Since

Power in = power available at the output port and coupled ports,

that is,

$$P_{in} = |b_4|^2 + |b_2|^2 . \qquad (3.33)$$

Summarizing the results of these two sections,

(i) for maximum coupling to the coupled port, $\ell = \lambda/4$ where λ is the effective wavelength in the directional coupler

(ii) for minimum coupling to the coupled port, $\ell = \lambda/2$

(iii) the coupled port (b_2) and the output port (b_4) are 90 degrees out of phase with respect to the signal outputs

(iv) the reflected waves at the input port (b_1) and the isolated port (b_3) are zero for matched loads.

Results (i) and (ii) are derived under the assumption that

$$\theta_{oe} = \theta_{oo} = \theta$$

and

$$Z_o = (Z_{oo}Z_{oe})^{1/2} .$$

3.4. A Microstrip Directional Coupler Design Procedure

This section in Chapter III gives the necessary and concluding design information for the fabrication of a microstrip directional coupler (Fig. 18). Two equations (3.34 and 3.35) are given that relate the even mode and odd mode impedances to the center conductor widths (w) and separation (s), conductor thickness (t), ground plane spacing (h), and dielectric substrate relative permittivity (ϵ_r).[7]

$$Z_{oo} = \frac{\eta/\sqrt{\epsilon_r}}{\frac{w}{h} + \frac{2}{3\sqrt{\epsilon_r}}\left[\frac{w}{h} - \left(\frac{1}{\frac{w}{h}+1}\right)^2\right] + \frac{1.35}{\log_{10}\frac{4h}{t}} + \frac{1.35}{\log_{10}\frac{4s}{\pi t}} + \frac{4}{3\sqrt{\epsilon_r}}\left(\frac{1}{\frac{s}{w}+1}\right)} \qquad (3.34)$$

where η = the free space impedance.

$$Z_{oe} = \frac{\eta/\sqrt{\epsilon_r}}{DEN} \tag{3.35}$$

where

$$DEN = \frac{w}{h} + \frac{1}{3\sqrt{\epsilon_r}}\left[\frac{w}{h} - \left(\frac{1}{\frac{w}{h}+1}\right)^2\right] + \frac{1.35}{\log\frac{4h}{t}}$$

$$+ \frac{1}{2}\left[\frac{w}{3h\sqrt{\epsilon_r}}\left(1 + \frac{1}{\frac{w}{s}+1}\right) - \frac{2}{3\sqrt{\epsilon_r}}\left(\frac{1}{\frac{w}{h}+1}\right)^2\right]$$

$$+ \frac{1}{2}\left[\frac{1.35}{\log_{10}\frac{4h}{t}}\left(1 + \frac{1}{\frac{w}{s}+1}\right)\right].$$

Using Eqs. (3.34) and (3.35) with Eqs. (3.27b) and (3.31), a design procedure for a microwave microstrip directional coupler can be formulated.

The basic design approach for a microstrip directional coupler is as follows:[7,8]

(i) Generate a set of curves from Eqs. (3.34) and (3.35) similar to those given in Fig. 19. A (t/h) ratio is predetermined from the fabrication method employed and a relative permittivity (ϵ_r) is determined by the dielectric substrate that is selected.

(ii) From the desired coupling in decibels, calculate the equivalent voltage coupling (K),

$$\text{db coupling} = 20 \log_{10} K.$$

(iii) From Eqs. (3.27b) and (3.31), Z_{oe} and Z_{oo} can be calculated.

(iv) With the calculated values for Z_{oo} and Z_{oe}, construct two horizontal lines on the generated curves corresponding to the derived Z_{oe} and Z_{oo} values.

(v) Construct a vertical line perpendicular to the two horizontal lines. Where this vertical line passes through the intersection of the two horizontal lines and equal valued separation curves (s/h), a simultaneous solution to Eqs. (3.34) and (3.35) is obtained. From this procedure the s/h and w/h ratios are known.

With the following determined quantities,

Z_o = system coupler impedance

Z_{oe}, Z_{oo} = even and odd mode impedances

K = voltage coupling coefficient

w/h = strip width to ground plane spacing ratio

s/h = strip separation to ground plane spacing ratio

θ = coupler electrical length,

a microstrip directional coupler can be fabricated. The coupler electrical length (θ) must be converted to physical length. It is assumed that the odd mode electrical length (θ_o) and even mode electrical length (θ_e) are equal. Then the physical length can be approximated as follows. Consider both microstrip lines in the coupling region of the directional coupler equal in length. The length of only one line then needs to be calculated.

From Fig. 7, the effective wavelength of the coupling section (λ_m) is expressed as a ratio with respect to the free space wavelength (λ_o).

CHAPTER IV

TESTING OF MICROSTRIP TRANSMISSION LINES AND DIRECTIONAL COUPLERS

4.1. Design Specifications

With respect to fabrication three particular areas were investigated. The first area entailed depositing a center conductor with the configuration as shown in Fig. 2. The dimensions used in this case were w = .025 inch and h = .025 inch. This design was to give a microstrip line with 50 ohms characteristic impedance.

In the second area of fabrication, microstrip bends, as shown in Fig. 12, were constructed. The width of the center conductor in these lines was w = .025 inch.

The construction of a microstrip directional coupler as in Fig. 18 comprised the third area of fabrication. The dimensions of the directional coupler were:

$s/h = .625$

$w/h = .96$ (in the coupling region)

$w/h = 1.0$ (elsewhere)

$\ell_c = .317$ inch (length of coupling region).

This directional coupler was designed to give a signal at the coupled port down 20 db in amplitude from the input signal.

4.2. Microstrip Transmission Line Data

The different microstrip lines and directional coupler were tested on a Hewlett-Packard 8542A automatic network analyzer. A description of the testing procedure is given in the operating and service manual for the HP 8542A.

A representative set of curves giving the pertinent data for the devices that were tested is shown in Fig. 20 and Tables I, II, and III.

Figure 20 gives the VSWR and insertion loss curves for the microstrip line shown in Fig. 2 with w/h = 1.0.

Three different strip width patterns were fabricated, all with their w/h ratio close to unity. The three widths (w) used were:

(i) w = .022 inch

(ii) w = .025 inch

(iii) w = .027 inch.

Table I shows the test results for three particular microstrip lines (Fig. 2) corresponding to the different widths. For the six frequencies indicated, the reflection coefficient (denoted as refl. = reflection coefficient amplitude and angle = the phase angle of the reflection coefficient), voltage standing wave ratio (VSWR), gain (insertion loss), and phase of the output signal are given (the phase of the input signal at the input boundary of the center conductor is the reference).

Table I. Test Data on Straight Microstrip Lines.

Freq MHz	Refl.	Angle	VSWR	Insertion loss db	Phase deg
		Line No. 1 -- w = .022 inch			
2700.000	.030	- 6.4	1.062	-.81	102.1
2800.000	.037	-19.5	1.077	-.78	92.7
2900.000	.043	-30.9	1.089	-.80	83.3
3000.000	.048	-40.3	1.101	-.96	72.4
3100.000	.054	-50.9	1.114	-.97	62.6
3199.999	.058	-59.3	1.123	-.91	53.6
		Line No. 2 -- w = .025 inch			
2700.000	.026	56.5	1.052	-.72	100.6
2800.000	.027	52.8	1.055	-.66	89.8
2900.000	.024	49.9	1.048	-.72	81.2
3000.000	.021	49.6	1.044	-.93	71.0
3100.000	.016	57.1	1.033	-.85	59.9
3199.999	.017	58.1	1.034	-.75	50.3
		Line No. 3 -- w = .027 inch			
2700.000	.008	-174.4	1.016	-.70	100.1
2800.000	.011	155.8	1.023	-.67	90.5
2900.000	.014	138.7	1.028	-.70	81.0
3000.000	.018	115.7	1.036	-.93	69.8
3100.000	.020	99.0	1.041	-.97	60.1
3199.999	.025	81.3	1.051	-.87	51.4

Table II gives the test results for the three different microstrip bends shown in Fig. 12. Table IIA refers to Fig. 12a, Table IIB to Fig. 12b, and Table IIC to Fig. 12c.

Table IIA. Microstrip with Gradual Bends.

Freq MHz	Refl.	Angle	VSWR	Insertion loss db	Phase deg
		Line No. 1			
2700.000	.028	97.0	1.058	-1.55	112.0
2800.000	.027	76.2	1.055	-1.55	103.3
2900.000	.024	50.3	1.050	-1.57	94.3
3000.000	.026	23.5	1.054	-1.69	83.8
3100.000	.031	- 1.7	1.063	-1.79	74.4
3199.999	.036	-20.5	1.074	-1.74	65.9
		Line No. 2			
2700.000	.040	-115.6	1.084	-1.05	97.5
2800.000	.036	-128.2	1.074	-1.03	87.8
2900.000	.030	-142.4	1.062	-1.06	78.1
3000.000	.022	-155.0	1.046	-1.28	66.9
3100.000	.015	-163.3	1.031	-1.33	57.1
3199.999	.007	-162.1	1.014	-1.25	48.2

Table IIB. Microstrip with Right Angle Bends.

Freq MHz	Refl.	Angle	VSWR	Insertion loss db	Phase deg
		Line No. 1			
2700.000	.044	- 73.0	1.092	- .93	101.8
2800.000	.043	- 86.4	1.089	- .90	92.1
2900.000	.041	- 99.2	1.086	- .94	82.7
3000.000	.038	-109.3	1.078	-1.15	71.7
3100.000	.036	-120.1	1.074	-1.18	61.9
3199.999	.033	-129.4	1.067	-1.11	52.8
		Line No. 2			
2700.000	.033	- 95.1	1.068	-1.08	101.7
2800.000	.031	-108.0	1.065	-1.05	92.1
2900.000	.030	-119.6	1.061	-1.07	82.7
3000.000	.025	-129.0	1.052	-1.29	71.7
3100.000	.023	-136.5	1.048	-1.31	62.0
3100.000	.020	-141.7	1.041	-1.23	53.0

Table IIC. Microstrip with 45-degree Bends.

Freq MHz	Refl.	Angle	VSWR	Insertion loss db	Phase deg
		Line No. 3			
2700.000	.029	17.6	1.060	- .94	134.3
2800.000	.025	.5	1.051	- .91	126.1
2900.000	.023	-18.4	1.046	- .92	117.9
3000.000	.020	-37.4	1.041	- .97	108.4
3100.000	.017	-58.9	1.035	-1.08	100.2
3199.999	.016	-88.1	1.033	-1.15	92.4
		Line No. 4			
2700.000	.032	41.1	1.066	- .97	134.7
2800.000	.027	28.8	1.055	- .93	126.4
2900.000	.022	13.0	1.045	- .94	118.2
3000.000	.018	- 3.3	1.037	- .98	108.7
3100.000	.014	-20.2	1.029	-1.07	100.5
3199.999	.009	-52.5	1.019	-1.14	92.7
		Line No. 5			
2700.000	.035	37.5	1.072	- .87	134.8
2800.000	.027	31.6	1.056	- .84	126.5
2900.000	.020	28.1	1.040	- .83	118.3
3000.000	.012	40.0	1.025	- .87	108.7
3100.000	.009	72.8	1.019	- .99	100.5
3199.999	.011	105.6	1.023	-1.04	92.8

Comparing the results given in Table II, it is seen that in general the 45-degree bends give the lowest VSWR with respect to the other two types of microstrip bends. The insertion loss is higher in the lines with bends than in the straight through lines.

4.3. Microstrip Directional Couplers Data

This section gives the results, in Tables IIIA to IIID, of the tests on one of the microstrip directional couplers that were fabricated. To establish suitable references, the four ports of the directional coupler are defined as follows:

Port 1, input port

Port 2, the coupled port

Port 3, the isolated port

Port 4, the direct output port.

Figure 18 can be used as a reference to locate the four ports for the directional coupler.

The data in Table III verifies that this directional coupler is symmetrical. The data is arranged in groups of three. The first grouping of three has port 1 as the input port and port 2 as the coupled port (Table IIIA). This follows from the original design of the coupler. The second grouping has port 2 as the input port and port 4 as the coupled port (Table IIID). The remaining data have ports 3 (Table IIIC) and 4 (Table IIID) as the input ports, respectively.

With port 1 as the input port, the coupled voltage signal at port 2 is down 15 db over the 500 MHz band with respect to the input signal amplitude and the signal at the isolated port is down 24 db. There was more than 1 db of loss between the input port and the output port. This is largely due to the lossy line; however, part of the input signal is coupled to ports 2 and 3. With port 4 as the input port, the corresponding results are almost the same as with port 1 as the input port.

Table IIIA. Microstrip Directional Coupler Test Data (Port 1 is input port).

Freq MHz	Refl.	Angle	VSWR	Insertion loss db	Phase deg
		Port 1 to Port 2			
2700.000	.012	154.8	1.024	-14.86	142.2
2725.000	.010	153.8	1.021	-14.89	139.4
2750.000	.009	152.1	1.018	-14.88	136.6
2775.000	.008	152.0	1.015	-14.90	133.5
2800.000	.006	149.7	1.013	-14.92	130.5
2825.000	.005	149.1	1.010	-14.91	127.7
2850.000	.003	143.4	1.007	-14.95	124.9
2875.000	.002	134.0	1.004	-14.97	122.5
2900.000	.001	114.8	1.002	-15.02	119.9
2925.000	.001	18.4	1.001	-15.05	116.7
2950.000	.002	- 8.4	1.004	-15.09	113.9
2975.000	.003	-17.9	1.005	-15.17	111.0
3000.000	.004	-20.7	1.007	-15.22	108.2
3025.000	.005	-28.4	1.010	-15.26	105.5
3050.000	.006	-31.5	1.011	-15.32	102.6
3075.000	.007	-34.2	1.013	-15.39	99.7
3100.000	.008	-39.2	1.016	-15.45	96.7
3125.000	.009	-41.3	1.019	-15.51	93.4
3150.000	.011	-45.2	1.021	-15.56	90.2
3175.000	.012	-47.3	1.024	-15.59	87.3
3199.999	.013	-49.1	1.027	-15.65	84.5

Table IIIA (Cont.).

Freq MHz	Refl.	Angle	VSWR	Insertion loss db	Phase deg
		Port 1 to Port 3			
2700.000	.012	132.6	1.024	-24.72	-30.9
2725.000	.011	127.5	1.022	-24.67	-34.2
2750.000	.010	124.4	1.020	-24.58	-37.3
2775.000	.009	120.5	1.018	-24.51	-40.4
2800.000	.008	116.8	1.016	-24.44	-43.6
2825.000	.006	109.1	1.013	-24.40	-46.8
2850.000	.005	102.5	1.011	-24.34	-49.9
2875.000	.004	88.6	1.009	-24.32	-53.0
2900.000	.004	70.4	1.007	-24.29	-56.0
2925.000	.004	46.9	1.007	-24.25	-58.9
2950.000	.004	27.6	1.008	-24.27	-62.2
2975.000	.005	10.8	1.010	-24.24	-65.4
3000.000	.006	.7	1.012	-24.25	-68.2
3025.000	.007	- 8.2	1.014	-24.22	-71.1
3050.000	.008	-14.0	1.016	-24.19	-74.1
3075.000	.009	-16.8	1.018	-24.17	-77.0
3100.000	.010	-22.4	1.020	-24.13	-79.9
3125.000	.011	-25.4	1.022	-24.12	-82.9
3150.000	.012	-29.1	1.023	-24.11	-86.1
3175.000	.012	-34.0	1.025	-24.13	-88.8
3199.999	.013	-37.1	1.027	-24.06	-91.7

Table IIIA (Concl.).

Freq MHz	Refl.	Angle	VSWR	Insertion loss db	Phase deg
		Port 1 to Port 4			
2700.000	.021	115.7	1.044	-1.32	135.1
2725.000	.020	110.9	1.042	-1.35	133.0
2750.000	.020	104.2	1.040	-1.34	131.2
2775.000	.018	100.5	1.037	-1.32	129.2
2800.000	.017	93.7	1.034	-1.28	127.0
2825.000	.016	85.1	1.032	-1.28	124.7
2850.000	.015	75.7	1.030	-1.33	122.7
2875.000	.014	65.4	1.029	-1.35	120.9
2900.000	.013	55.0	1.027	-1.30	119.0
2925.000	.013	45.6	1.027	-1.26	116.9
2950.000	.015	31.1	1.030	-1.24	114.2
2975.000	.014	23.5	1.029	-1.30	111.8
3000.000	.015	16.7	1.030	-1.37	109.8
3025.000	.016	11.7	1.033	-1.40	107.9
3050.000	.017	4.5	1.035	-1.43	105.9
3075.000	.018	- 2.6	1.037	-1.45	103.9
3100.000	.019	- 8.6	1.040	-1.46	101.8
3125.000	.020	-14.1	1.040	-1.51	99.6
3150.000	.020	-18.2	1.041	-1.59	97.8
3175.000	.023	-24.5	1.046	-1.55	96.1
3199.999	.023	-30.8	1.048	-1.49	94.0

Table IIIB. Microstrip Directional Coupler Test Data (Port 2 is input port).

Freq MHz	Refl.	Angle	VSWR	Insertion loss db	Phase deg
		Port 2 to Port 1			
2700.000	.060	9.9	1.127	-14.88	142.8
2725.000	.064	5.9	1.137	-14.87	140.2
2750.000	.068	1.5	1.146	-14.83	137.3
2775.000	.072	- 2.3	1.155	-14.81	134.1
2800.000	.075	- 5.8	1.163	-14.85	130.8
2825.000	.079	- 9.8	1.172	-14.93	128.1
2850.000	.083	-13.5	1.180	-14.98	125.5
2875.000	.086	-17.3	1.188	-15.00	123.4
2900.000	.089	-21.2	1.196	-14.98	120.4
2925.000	.092	-24.8	1.203	-15.00	117.4
2950.000	.096	-29.2	1.212	-15.06	114.3
2975.000	.098	-33.0	1.218	-15.14	111.4
3000.000	.101	-37.1	1.224	-15.21	108.8
3025.000	.104	-41.1	1.233	-15.19	106.1
3050.000	.107	-45.3	1.239	-15.21	103.2
3075.000	.109	-49.5	1.245	-15.24	99.9
3100.000	.111	-53.6	1.249	-15.30	96.6
3125.000	.112	-58.0	1.253	-15.39	93.7
3150.000	.113	-62.1	1.255	-15.44	91.0
3175.000	.114	-66.6	1.258	-15.41	88.0
3199.999	.115	-70.9	1.260	-15.43	84.8

Table IIIB (Cont.).

Freq MHz	Refl.	Angle	VSWR	Insertion loss db	Phase deg
		Port 2 to Port 4			
2700.000	.053	-21.5	1.111	-26.20	-29.7
2725.000	.055	-25.1	1.117	-26.16	-32.3
2750.000	.058	-28.3	1.124	-26.06	-34.9
2775.000	.061	-32.7	1.131	-25.92	-37.7
2800.000	.064	-36.0	1.137	-25.84	-40.5
2825.000	.067	-39.0	1.143	-25.76	-43.3
2850.000	.069	-42.2	1.148	-25.69	-46.0
2875.000	.072	-45.5	1.155	-25.62	-48.5
2900.000	.074	-48.8	1.160	-25.54	-51.2
2925.000	.077	-51.9	1.167	-25.41	-54.0
2950.000	.080	-55.1	1.173	-25.35	-57.2
2975.000	.082	-58.1	1.178	-25.32	-60.1
3000.000	.084	-61.5	1.184	-25.28	-62.7
3025.000	.086	-66.0	1.188	-25.19	-65.3
3050.000	.087	-69.7	1.192	-25.12	-68.2
3075.000	.089	-72.2	1.195	-25.02	-70.9
3100.000	.091	-75.8	1.200	-24.93	-73.7
3125.000	.092	-78.7	1.202	-24.85	-76.5
3150.000	.093	-82.3	1.206	-24.76	-79.1
3175.000	.095	-85.6	1.211	-24.66	-81.7
3199.999	.097	-89.1	1.214	-24.53	-84.7

Table IIIB (Concl.).

Freq MHz	Refl.	Angle	VSWR	Insertion loss db	Phase deg
		Port 2 to Port 3			
2700.000	.046	-11.9	1.096	-2.35	-33.9
2725.000	.049	-15.0	1.103	-2.37	-37.4
2750.000	.053	-18.9	1.111	-2.36	-40.9
2775.000	.056	-23.1	1.119	-2.36	-44.3
2800.000	.060	-26.7	1.128	-2.31	-47.9
2825.000	.063	-29.7	1.134	-2.35	-51.5
2850.000	.066	-32.7	1.142	-2.37	-55.4
2875.000	.070	-36.4	1.151	-2.38	-58.4
2900.000	.074	-40.5	1.159	-2.37	-62.0
2925.000	.077	-43.8	1.168	-2.34	-65.6
2950.000	.081	-47.0	1.176	-2.32	-69.6
2975.000	.083	-50.6	1.182	-2.35	-73.4
3000.000	.086	-53.8	1.189	-2.41	-77.0
3025.000	.089	-58.2	1.195	-2.45	-80.5
3050.000	.092	-61.9	1.202	-2.47	-84.0
3075.000	.094	-65.6	1.208	-2.48	-87.8
3100.000	.097	-68.6	1.215	-2.48	-91.5
3125.000	.099	-73.0	1.219	-2.53	-95.3
3150.000	.101	-76.7	1.224	-2.55	-99.0
3175.000	.104	-80.7	1.233	-2.53	-102.5
3199.999	.106	-84.8	1.237	-2.50	-106.3

Table IIIC. Microstep Directional Coupler Test Data (Port 3 is input port).

Freq MHz	Refl.	Angle	VSWR	Insertion loss db	Phase deg
		Port 3 to Port 4			
2700.000	.053	-22.2	1.112	-14.76	145.2
2725.000	.056	-25.0	1.118	-14.78	142.4
2750.000	.059	-27.6	1.126	-14.78	139.8
2775.000	.063	-30.8	1.134	-14.75	136.9
2800.000	.066	-33.3	1.141	-14.77	133.9
2825.000	.069	-35.5	1.147	-14.78	131.0
2850.000	.071	-37.9	1.154	-14.81	128.3
2875.000	.074	-40.6	1.160	-14.84	125.8
2900.000	.077	-43.2	1.166	-14.85	123.5
2925.000	.080	-45.6	1.173	-14.84	120.5
2950.000	.082	-48.1	1.179	-14.91	117.4
2975.000	.084	-50.5	1.185	-14.97	114.7
3000.000	.087	-53.0	1.190	-15.02	111.9
3025.000	.089	-56.4	1.195	-15.08	109.3
3050.000	.091	-59.2	1.199	-15.13	106.7
3075.000	.092	-61.4	1.203	-15.22	103.8
3100.000	.094	-64.2	1.208	-15.24	100.9
3125.000	.096	-66.1	1.213	-15.33	98.2
3150.000	.098	-68.9	1.217	-15.34	95.0
3175.000	.100	-71.5	1.222	-15.35	92.3
3199.999	.102	-74.0	1.227	-15.32	89.3

Table IIIC (Cont.).

Freq MHz	Refl.	Angle	VSWR	Insertion loss db	Phase deg
		Port 3 to Port 1			
2700.000	.059	10.1	1.126	-24.73	-30.2
2725.000	.064	6.5	1.136	-24.64	-33.1
2750.000	.068	2.5	1.147	-24.51	-36.4
2775.000	.073	- .8	1.157	-24.44	-39.8
2800.000	.077	- 3.8	1.168	-24.40	-43.4
2825.000	.082	- 7.3	1.179	-24.41	-46.4
2850.000	.086	-10.4	1.188	-24.42	-49.1
2875.000	.089	-13.6	1.196	-24.33	-52.0
2900.000	.093	-16.8	1.206	-24.26	-55.0
2925.000	.097	-20.1	1.214	-24.22	-58.2
2950.000	.101	-23.6	1.224	-24.23	-61.6
2975.000	.103	-27.2	1.231	-24.24	-64.6
3000.000	.106	-30.8	1.236	-24.23	-67.3
3025.000	.109	-34.2	1.245	-24.15	-70.1
3050.000	.112	-38.0	1.252	-24.09	-73.2
3075.000	.114	-41.4	1.258	-24.07	-76.4
3100.000	.117	-45.2	1.264	-24.06	-79.3
3125.000	.119	-48.9	1.269	-24.05	-82.2
3150.000	.120	-52.4	1.273	-24.03	-84.9
3175.000	.122	-56.1	1.277	-23.96	-87.8
3199.999	.123	-59.7	1.280	-23.90	-91.1

Table IIIC (Concl.).

Freq MHz	Refl.	Angle	VSWR	Insertion loss db	Phase deg
		Port 3 to Port 2			
2700.000	.052	3.2	1.110	-2.36	-33.6
2725.000	.056	.8	1.120	-2.41	-37.1
2750.000	.060	- 2.9	1.127	-2.35	-40.4
2775.000	.063	- 4.8	1.135	-2.32	-44.0
2800.000	.066	- 6.0	1.142	-2.30	-47.8
2825.000	.072	- 8.4	1.156	-2.37	-51.5
2850.000	.076	-10.8	1.165	-2.43	-55.0
2875.000	.080	-13.7	1.173	-2.46	-58.2
2900.000	.083	-16.9	1.181	-2.43	-61.6
2925.000	.086	-19.2	1.187	-2.40	-65.3
2950.000	.091	-21.6	1.200	-2.42	-69.2
2975.000	.094	-24.8	1.208	-2.51	-72.8
3000.000	.097	-28.1	1.216	-2.53	-76.2
3025.000	.102	-31.5	1.226	-2.54	-79.6
3050.000	.105	-34.9	1.234	-2.50	-83.0
3075.000	.108	-38.0	1.242	-2.50	-86.9
3100.000	.110	-41.0	1.248	-2.48	-91.0
3125.000	.113	-44.4	1.254	-2.54	-94.7
3150.000	.115	-47.2	1.260	-2.59	-98.3
3175.000	.118	-50.8	1.267	-2.51	-101.8
3199.999	.120	-54.1	1.272	-2.46	-105.6

Table IIID. Microstrip Directional Coupler Test Data (Port 4 is input port).

Freq MHz	Refl.	Angle	VSWR	Insertion loss db	Phase deg
		Port 4 to Port 3			
2700.000	.031	44.9	1.063	-14.82	145.1
2725.000	.033	40.5	1.068	-14.80	142.4
2750.000	.035	35.8	1.073	-14.80	139.5
2775.000	.037	32.0	1.078	-14.83	136.7
2800.000	.040	29.4	1.083	-14.83	133.8
2825.000	.042	25.8	1.088	-14.87	131.1
2850.000	.045	22.8	1.094	-14.93	128.4
2875.000	.047	19.4	1.098	-14.94	126.2
2900.000	.049	16.8	1.104	-14.96	123.4
2925.000	.051	14.1	1.108	-15.00	120.8
2950.000	.054	10.5	1.113	-15.06	117.8
2975.000	.056	7.9	1.118	-15.12	115.0
3000.000	.058	5.2	1.122	-15.16	112.3
3025.000	.059	2.0	1.126	-15.22	109.7
3050.000	.061	- 1.0	1.131	-15.23	107.1
3075.000	.064	- 3.7	1.136	-15.26	104.3
3100.000	.066	- 6.3	1.140	-15.29	101.3
3125.000	.068	- 9.1	1.146	-15.36	98.0
3150.000	.070	-11.5	1.150	-15.41	95.2
3175.000	.071	-14.0	1.152	-15.45	92.6
3199.999	.072	-16.1	1.155	-15.46	89.8

Table IIID (Cont.).

Freq MHz	Refl.	Angle	VSWR	Insertion loss db	Phase deg
		Port 4 to Port 2			
2700.000	.033	47.0	1.068	-26.31	-30.2
2725.000	.035	42.9	1.073	-26.20	-32.4
2750.000	.037	38.4	1.077	-26.09	-35.1
2775.000	.039	34.5	1.081	-26.00	-37.9
2800.000	.041	32.0	1.087	-25.93	-40.6
2825.000	.044	28.3	1.092	-25.87	-43.2
2850.000	.046	25.5	1.096	-25.82	-45.8
2875.000	.048	22.2	1.100	-25.76	-49.1
2900.000	.050	19.6	1.105	-25.66	-51.7
2925.000	.052	16.9	1.110	-25.58	-54.4
2950.000	.054	13.1	1.114	-25.54	-57.1
2975.000	.055	10.7	1.117	-25.49	-59.9
3000.000	.057	8.0	1.121	-25.40	-62.6
3025.000	.059	4.8	1.125	-25.34	-65.1
3050.000	.060	1.6	1.129	-25.22	-67.8
3075.000	.062	- 1.1	1.133	-25.10	-70.6
3100.000	.064	- 3.7	1.136	-24.98	-73.5
3125.000	.066	- 6.6	1.142	-24.92	-76.6
3150.000	.068	- 8.8	1.145	-24.90	-79.6
3175.000	.069	-11.6	1.147	-24.80	-82.0
3199.999	.070	-13.9	1.150	-24.65	-84.8

Table IIID (Concl.).

Freq MHz	Refl.	Angle	VSWR	Insertion loss db	Phase deg
		Port 4 to Port 1			
2700.000	.023	59.8	1.046	-1.34	135.5
2725.000	.025	54.7	1.051	-1.32	133.8
2750.000	.025	49.3	1.052	-1.24	131.9
2775.000	.027	46.0	1.055	-1.17	129.4
2800.000	.030	44.4	1.063	-1.21	126.7
2825.000	.034	39.3	1.070	-1.31	124.6
2850.000	.036	37.3	1.075	-1.37	122.9
2875.000	.039	34.5	1.080	-1.38	121.3
2900.000	.041	32.5	1.084	-1.32	119.3
2925.000	.043	30.4	1.090	-1.29	117.0
2950.000	.046	25.1	1.098	-1.32	114.4
2975.000	.048	22.1	1.101	-1.42	112.4
3000.000	.050	20.8	1.104	-1.48	110.9
3025.000	.052	17.5	1.110	-1.43	109.2
3050.000	.054	13.2	1.115	-1.38	107.2
3075.000	.056	10.1	1.119	-1.34	104.7
3100.000	.058	7.6	1.122	-1.38	102.1
3125.000	.059	5.5	1.126	-1.50	100.1
3150.000	.062	3.5	1.132	-1.51	98.4
3175.000	.065	- .0	1.139	-1.45	96.5
3199.999	.066	-2.3	1.142	-1.38	93.8

However, with ports 2 and 3 as the input ports, there is considerable loss between the input and direct output ports. This loss is 1 db higher than when ports 1 and 4 were the input ports and can be attributed to a faulty transmission line along the port 2 and 3 side of the coupler. Thus the transmission line on this side of the coupler needs to be redesigned. The coupler behaves in the contradirectional sense as was intended. The degree of coupling can be altered by changing the (s/h) ratio and the length of the coupling section. The phase difference between the two signals at the coupled and output ports is not 90 degrees as predicted by Eq. (3.30). This is a result of two things: $\theta_e \neq \theta_o$, and the coupling length not being one-fourth of a wavelength. The directivity for this coupler was essentially 10 db over the frequency bandwidth that the tests were performed at. The data given for this directional coupler was typical of all the directional couplers that were fabricated. These couplers gave uniform test results.

The difference between the predicted and observed coupling to the coupled and isolated ports can be minimized by improving the calculation of the voltage coupling (K). This can be done by more adequately predicting the electrical lengths of the even (θ_e) and odd modes (θ_o). This will change the value of K and subsequently the w/h and s/h ratios as well as the length of the coupling region.

The predicted insertion loss between ports 1 and 4 from Eq. (3.32) is 1.01 db. This loss is for the coupler itself and does not include the loss in the transmission lines leading from

the coupler to the edge of the substrate. The measured total loss was 1.37 db at 3 GHz, the design frequency. The .36 db difference between the calculated and measured value can be accounted for by the loss in the lines leading to and from the coupler. For a 1-inch line, the insertion loss was about 1.05 db at 3 GHz, as shown in Fig. 20. The total length of lead-in lines to the coupler (Fig. 18) was about .40 inch, and correspondingly from the measurements taken the insertion loss would be about .4 db. This .4 db could easily account for the .36 db difference between the measured and calculated values of insertion loss for the directional coupler.

4.4. Summary

The objective of this report was to establish strict guidelines in the design of a microwave microstrip transmission line, and then use the microstrip line techniques to design and fabricate a directional coupler.

Equations (1.1) and (1.2) give the desired geometry of the microstrip line for a desired characteristic impedance. Figure 9 gives a relationship between the microstrip line effective wavelength and free space wavelength. The accuracy of Eqs. (1.1) and (1.2) is verified by the results given in Table I for a straight microstrip line. More work needs to be done on the thick film fabrication procedure in order to reduce the insertion loss.

The microstrip bends shown in Fig. 12 will perform satisfactorily at microwave frequencies up to 15 GHz. Table II shows

that these bends have VSWR measurements of the same order of magnitude as straight lines.

A microstrip directional coupler can be designed by using Eqs. (3.27b), (3.30b), (3.34), and (3.35). Table III gives the test results of a directional coupler. The directional coupler exhibited the symmetrical property predicted. However, the output signal at the coupled and direct output ports did not differ 90 degrees in phase. This is a result of not having equal electrical lengths for the even and odd modes. Also a severe mismatch occurred between ports 2 and 3. This mismatch can be attributed to the bend adjacent to the directional coupler on the port 3 side having a nonuniform width along two lines in the bend. Since all the directional couplers were fabricated from the same screen, they all had the same flaw.

Basically, center conductor strip widths can be held to a tolerance of at least $\pm$.001 inch and possibly to a closer tolerance than this. It was also learned that the motion of the squeegee in printing should be in the direction of the longest dimension of the center conductor.

For the pattern configuration as shown in Fig. 2, there are only two possible directions for the squeegee to move when printing. However, for a directional coupler, as shown in Fig. 18, there are eight conductor path segments. Although the lines leading to and from the coupler can change, the parallel lines that form the coupling region are critically fixed by the design constraints. Therefore the motion of the squeegee should be in the direction of these two parallel lines.

In conclusion, a few brief comments should be made regarding the thin film process, a possible alternative to thick film fabrication. The thin film procedure does promise better dimensional tolerance control than does thick film. However, in the light of present-day production capability and costs, the thick film procedure is superior.

The following is a brief account of some precautions that should be followed when fabricating thick film circuits. The selection of a conductor paste should be compatible with the particular fabrication process. The conductor properties are affected by the choice of printing and firing techniques. In fact, two different users of the same conductor paste will obtain different results. A test program should be set up to determine the conductor paste which is best suited for the particular application and processing procedure.

If a conductor paste performs poorly, this may be due to subtle variations in the printing and firing procedure. A given conductor paste gives uniform results only on a given run. In the next fabrication run, the results may be uniform but not necessarily consistent with the previous run. Repeatable results can be obtained only if the entire process is exactly the same each and every time.

A precise account should be made of every step of the fabrication process. For example, the same screen and squeegee combinations must be used every time; also the angle of attack of the squeegee on the screen must not vary. Time and temperature firing profiles should be taken and held constant once an

optimum is achieved. The tension of the printing screen must be continuously monitored as screens lose their tension with repeated use, causing the printed conductor to lose its sharp edge and consistency of thickness.

Also, conductor paste viscosity must be the same from printing to printing if consistent results are required. It has been noted that even five-degree temperature excursions will cause viscosity variations that shift the value of resistivity as must as 50 per cent.[10] Hence all paste work, storage, blending, and printing should be done in the same area and this area should have an environment that is controlled as tightly as possible.

In the Electrical Engineering solid-state laboratory at Kansas State University these various precautions above were often impossible to follow because of economic considerations and the availability of the laboratory to everyone. Considering the overall aspect of the project and the results, the project should be termed a reasonable success.

ACKNOWLEDGMENTS

I wish to express my gratitude to my major advisor, Dr. D. E. Kaufman, for his guidance. My appreciation is also given to Dr. G. L. Johnson and Mr. J. L. Taylor for their encouragement.

I wish also to thank Mrs. F. M. Crawford for her secretarial assistance, and my wife for her continued patience and understanding.

This report is dedicated to my mother and father, both of whom made my educational opportunities possible, and to Mr. J. L. Taylor for this stimulation and close guidance while working with the Bendix Corporation.

REFERENCES

1. H. A. Wheeler, "Transmission Line Properties of Parallel Wide Strips by a Conformal-Mapping Approximation," IEEE Trans. Microwave Theory and Techniques, May, 1964, Vol. MTT-12, No. 3, pp. 280-288.

2. H. A. Wheeler, "Transmission Line Properties of Parallel Strips Separated by a Dielectric Sheet," IEEE Trans. Microwave Theory and Techniques, March, 1965, Vol. MTT-13, No. 2, pp. 172-185.

3. M. Caulton, J. J. Hughes, H. Sobol, "Measurements on the Properties of Microstrip Transmission Lines for Microwave Integrated Circuits," RCA Review, September, 1966, Vol. 17, No. 3, pp. 377-391.

4. G. D. Vendelin, "High Dielectric Substrates for Microwave Hybrid Integrated Circuitry," IEEE Trans. Microwave Theory and Techniques, December, 1967, Vol. MTT-15, No. 12, pp. 750-751.

5. Microwave Engineers Technical and Buyers Guide Edition, Microwave Journal International, February, 1969, p. 66.

6. A. Schwarzmann, "Microwave Plus Equations Adds Up to Fast Designs," Electronics, October 2, 1967, pp. 109-112.

7. A. Schwarzmann, "Approximate Solutions for a Coupled Pair of Microstrip Lines in Microwave Integrated Circuits," Microwave Journal, May, 1969, Vol. 12, No. 5, pp. 79-82.

8. R. Seckelman, "On Measurements of Microstrip Properties," Microwave Journal, January, 1968, Vol. 11, No. 2, pp. 61-64.

9. R. Levy, "Directional Couplers," Advances in Microwaves, Vol. 1, pp. 115-206, 1966.

10. W. G. Dryden, "Achieving Consistent Results with Thick Film," Solid State Technology, September, 1971, Vol. 14, No. 9, pp. 54-57.

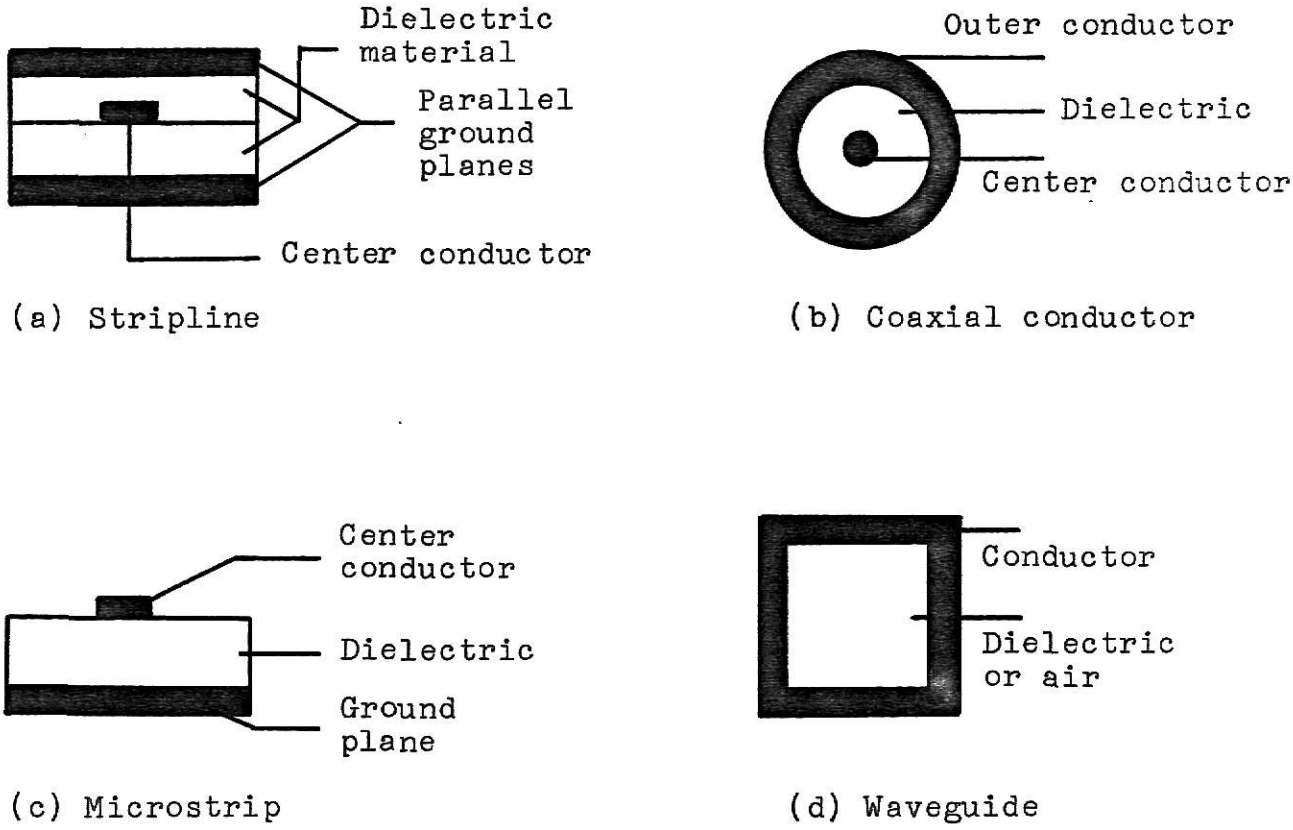

Fig. 1. Various microwave transmission lines (longitudinal view).

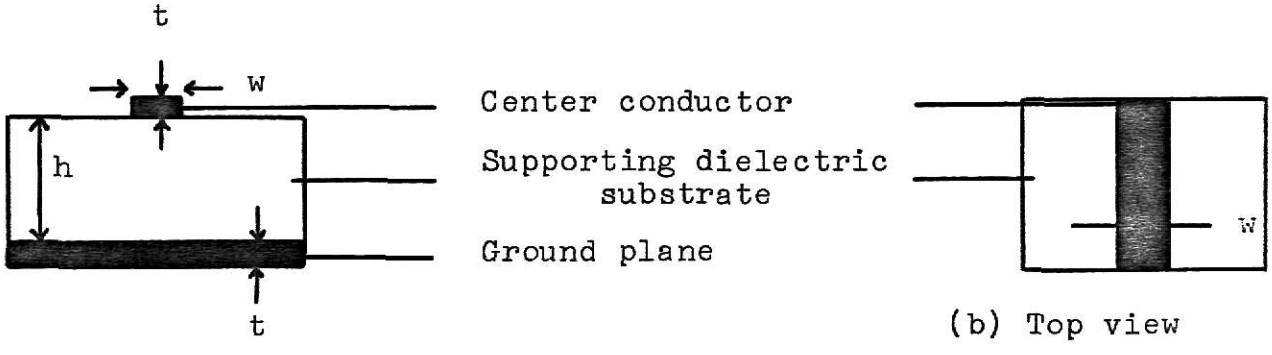

Fig. 2. Detailed microstrip line.

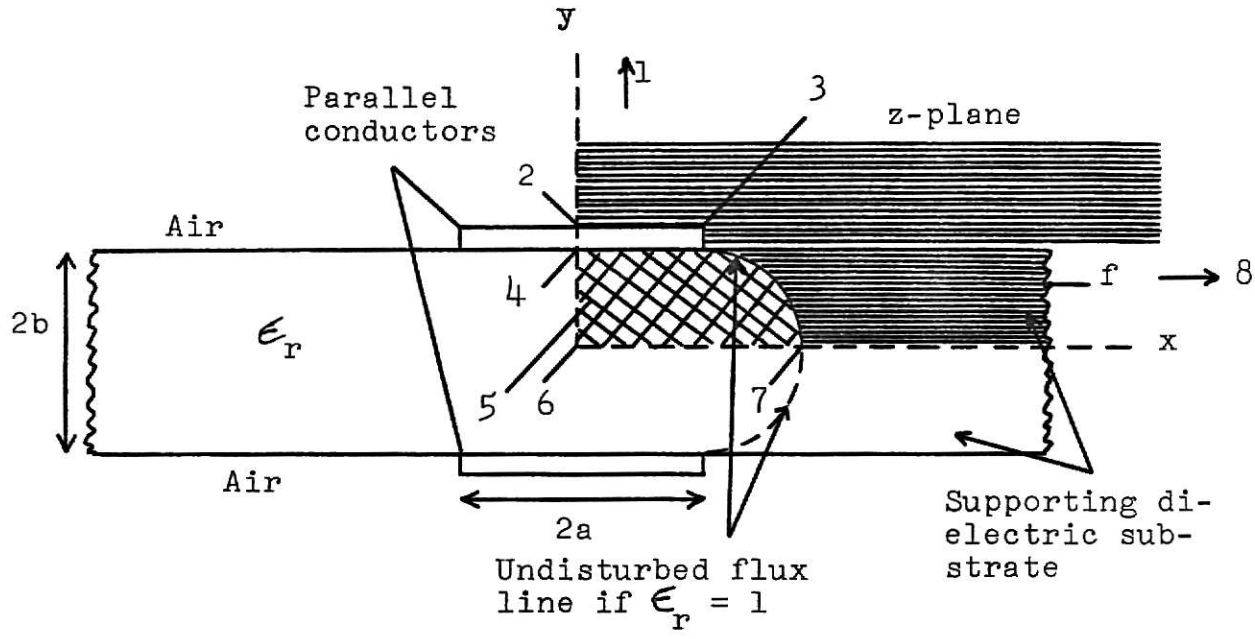

Fig. 3. Wheeler's original parallel plane waveguide.

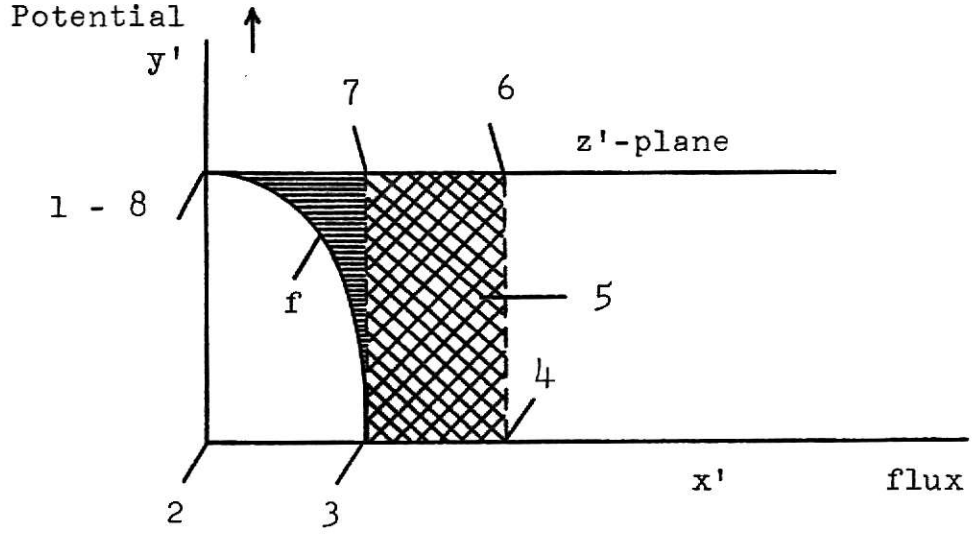

Fig. 4. Mapping of the indicated quadrant of Fig. 3.

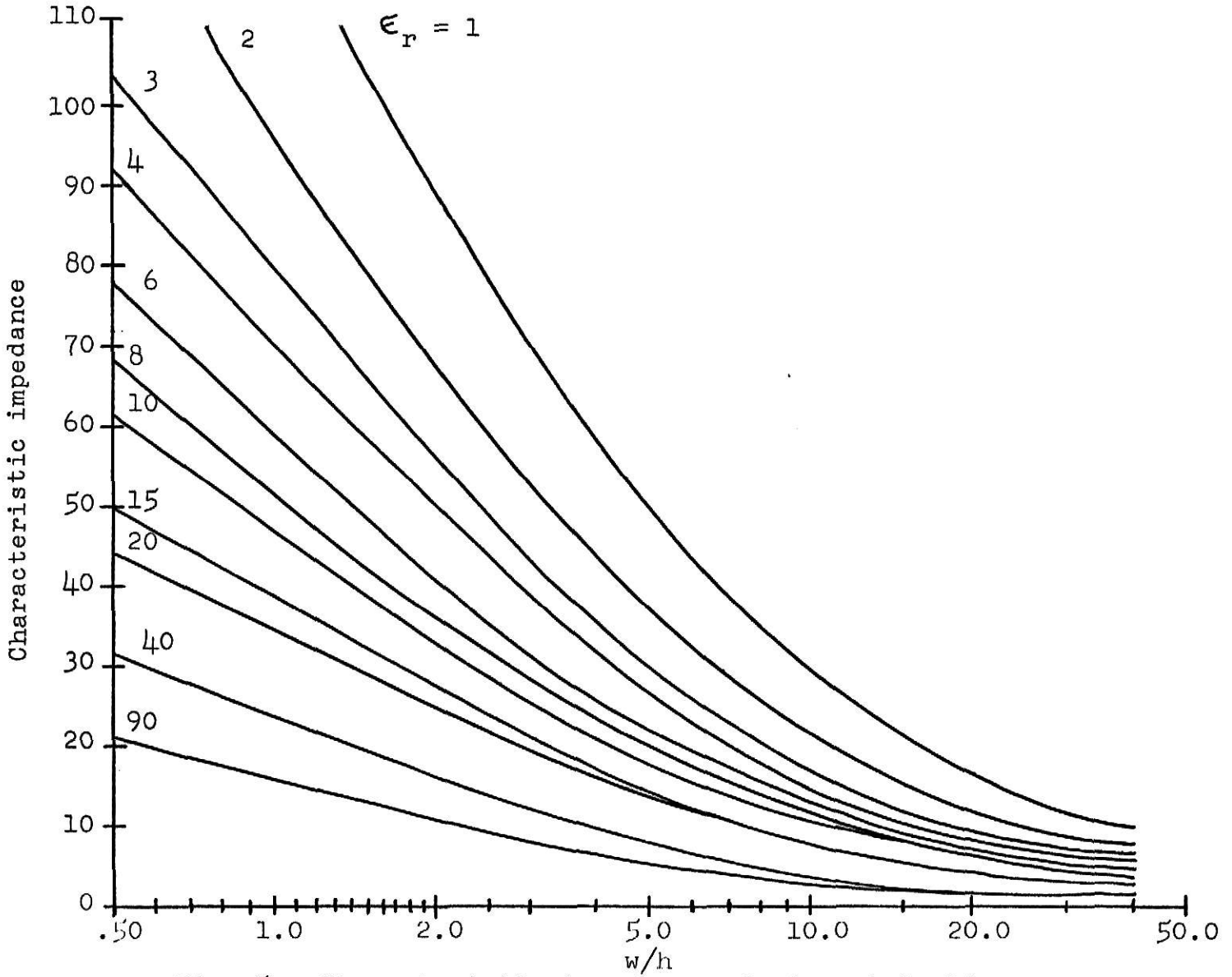

Fig. 5. Characteristic impedance of microstrip lines--wide strip approximation ($w/h > 1.0$).

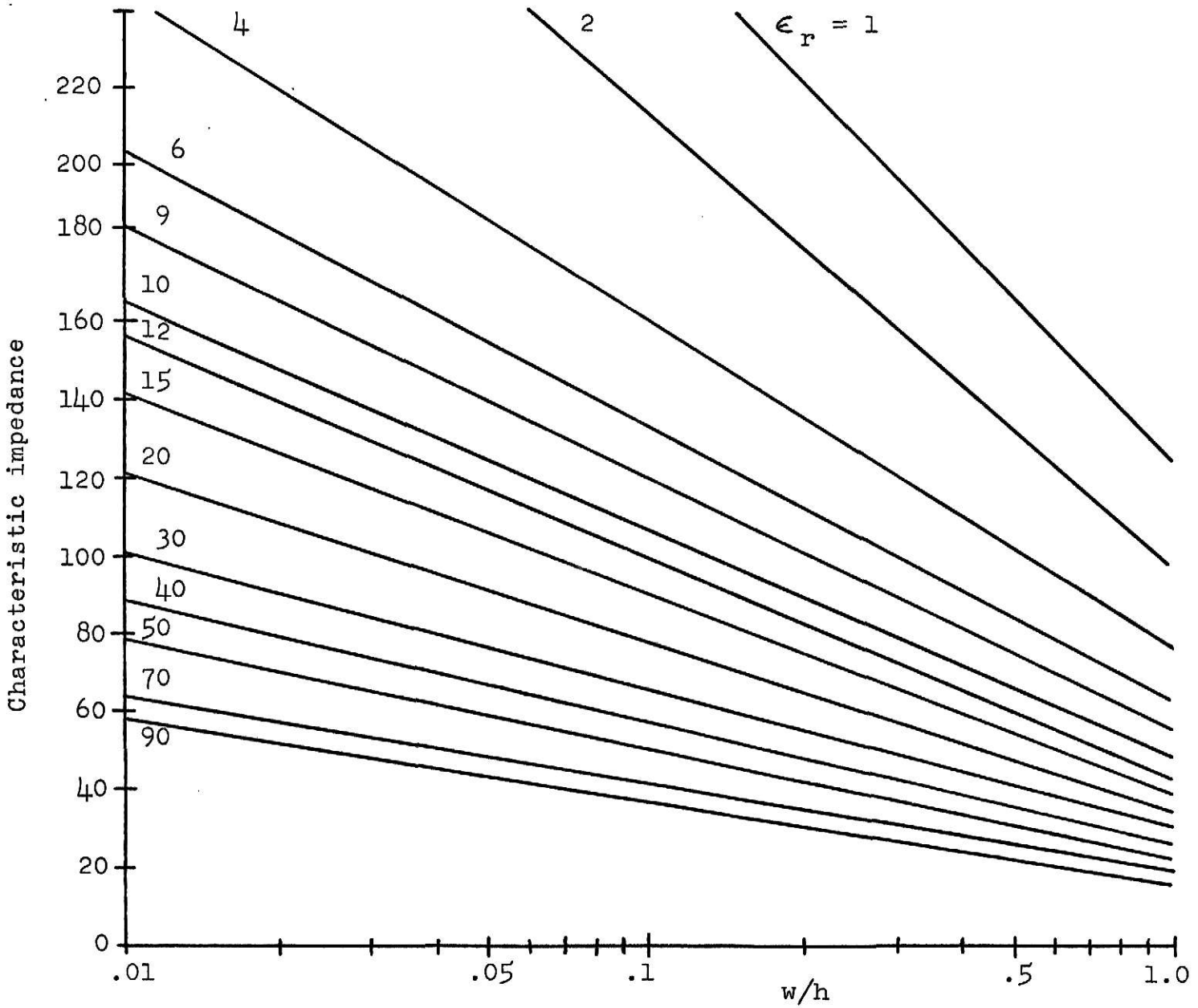

Fig. 6. Characteristic impedance of microstrip line--narrow strip approximation (w/h < 1.0).

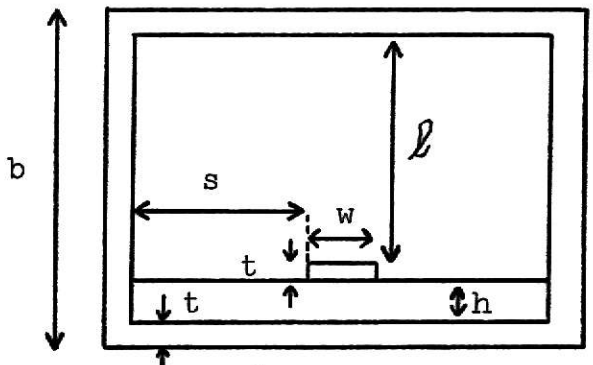

ϵ_r = 8.875; h = .020"; ℓ + t + h = .300"; 2s + w = .500"

Fig. 7. Enclosed microstrip (5).

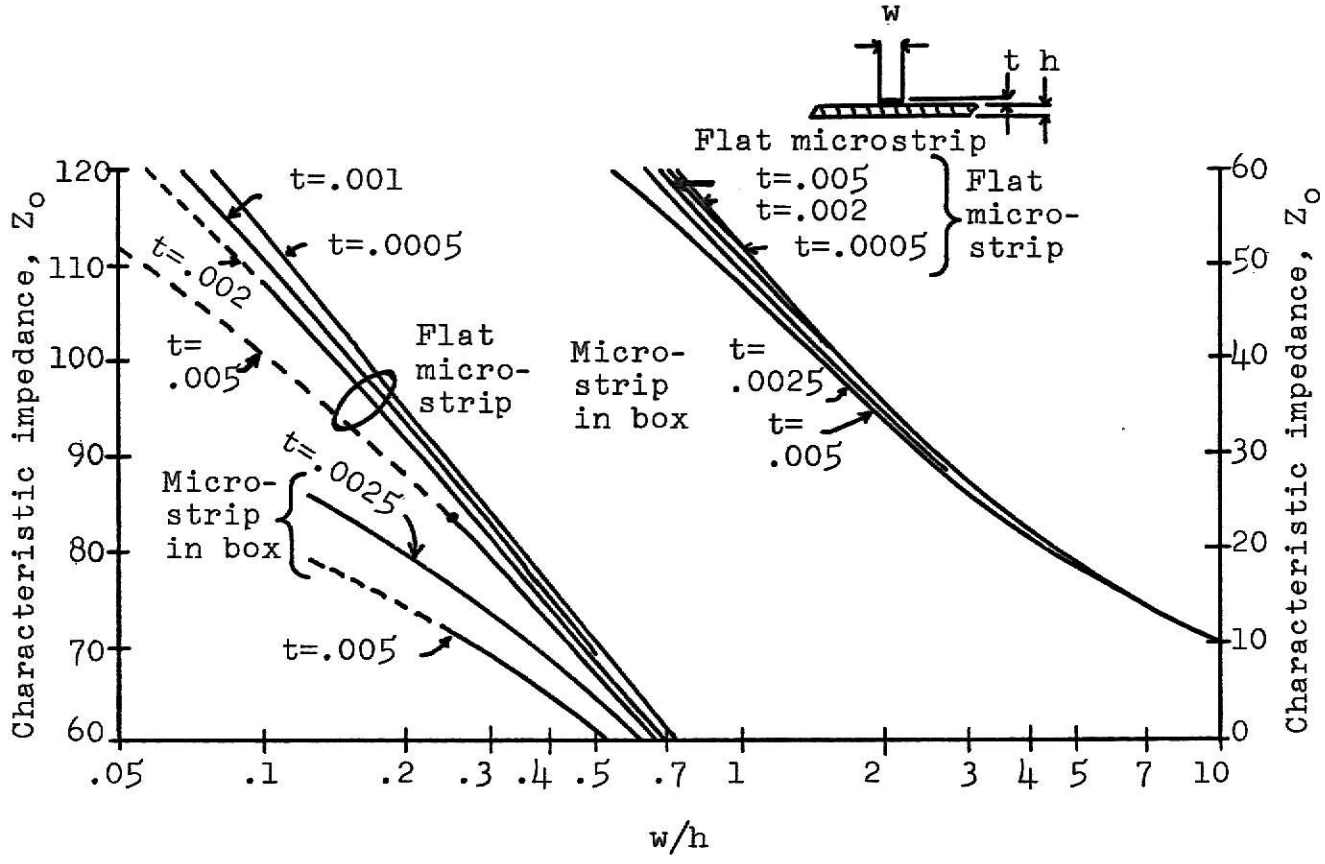

Fig. 8. Characteristic impedance of enclosed and open microstrip lines (5).

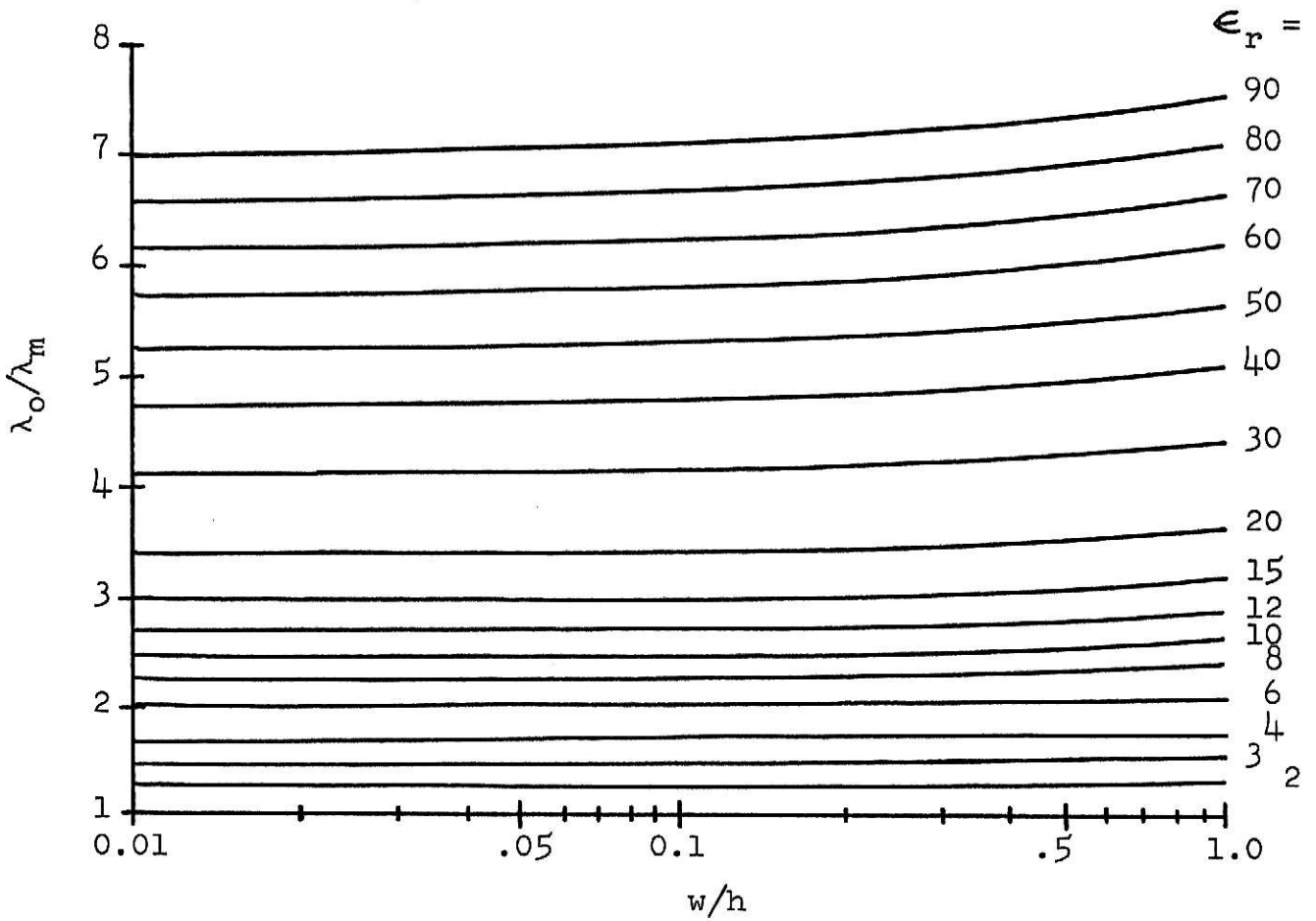

Fig. 9. Ratio of free space wavelength (λ_o) to microstrip wavelength (λ_m) (5).

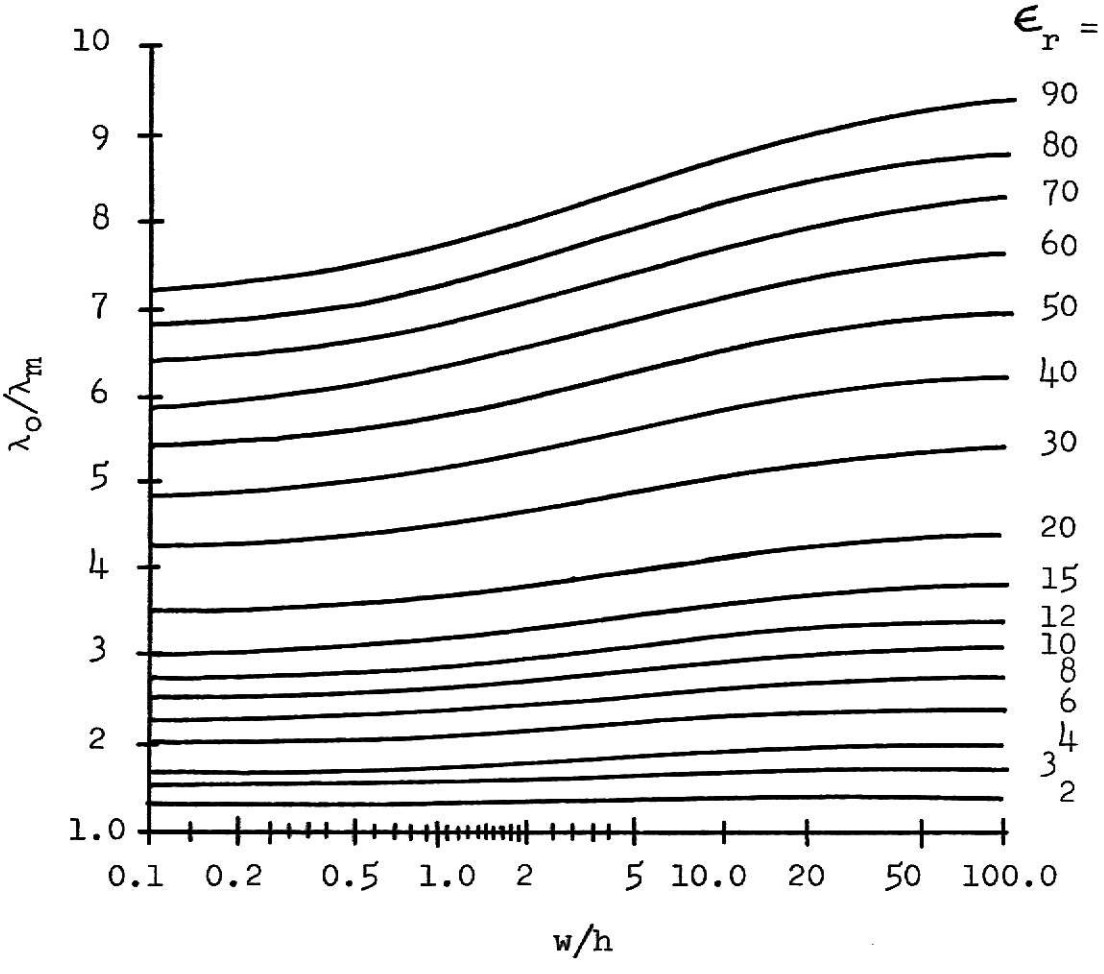

Fig. 9. Continued.

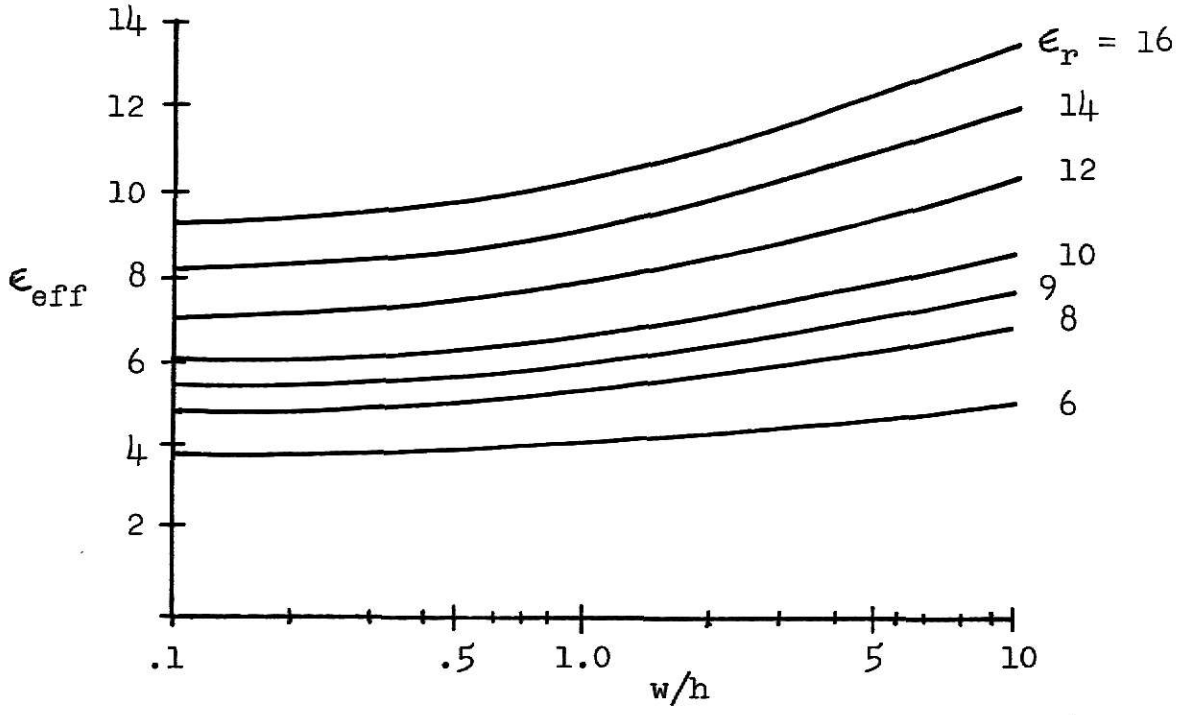

Fig. 10. Microstrip effective dielectric constant (7).

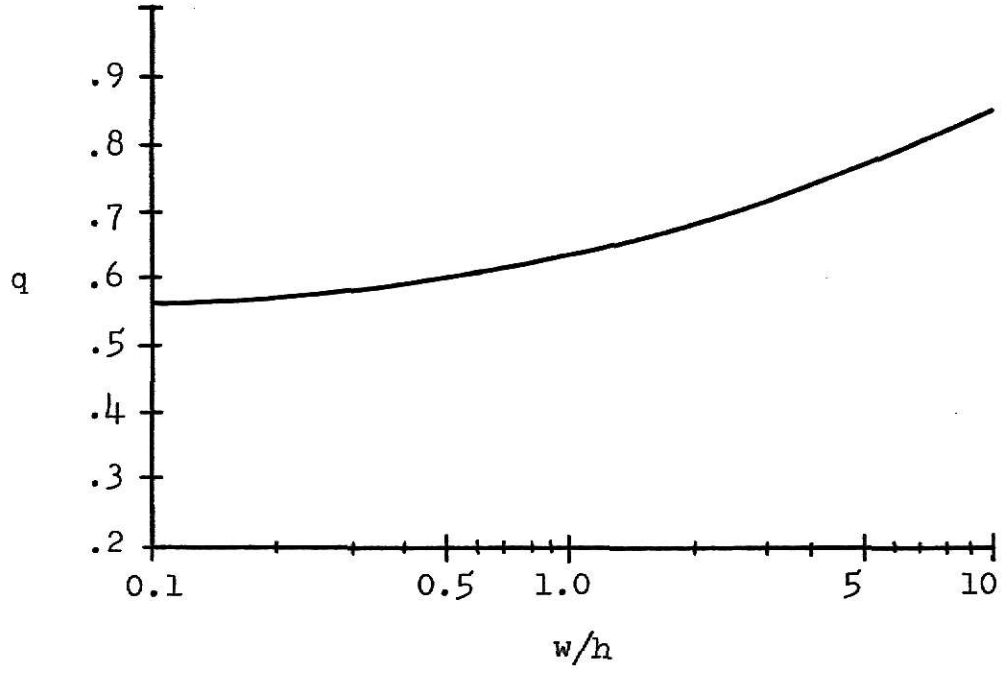

Fig. 11. Microstrip filling fraction (7).

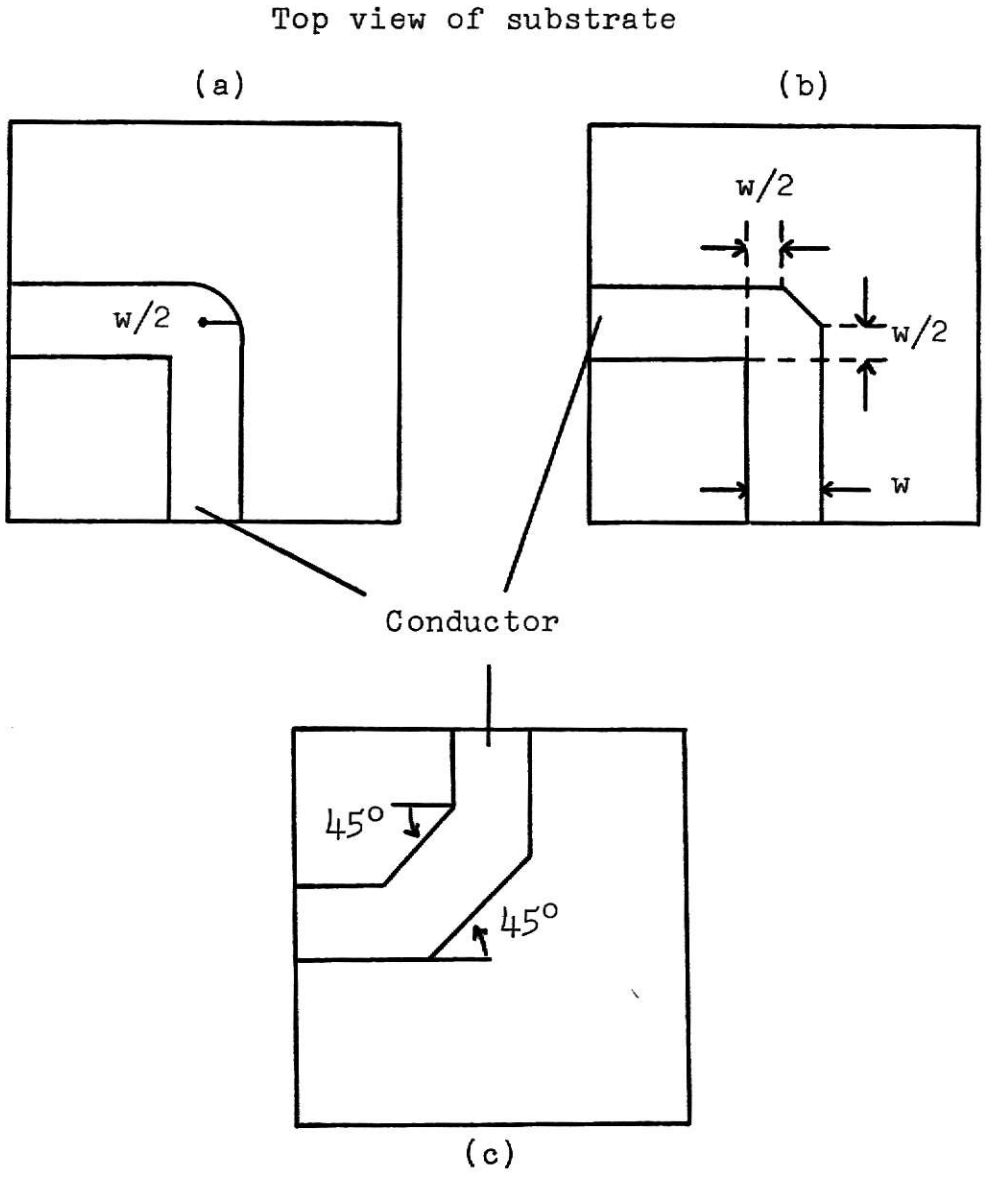

Fig. 12. Microstrip bends.

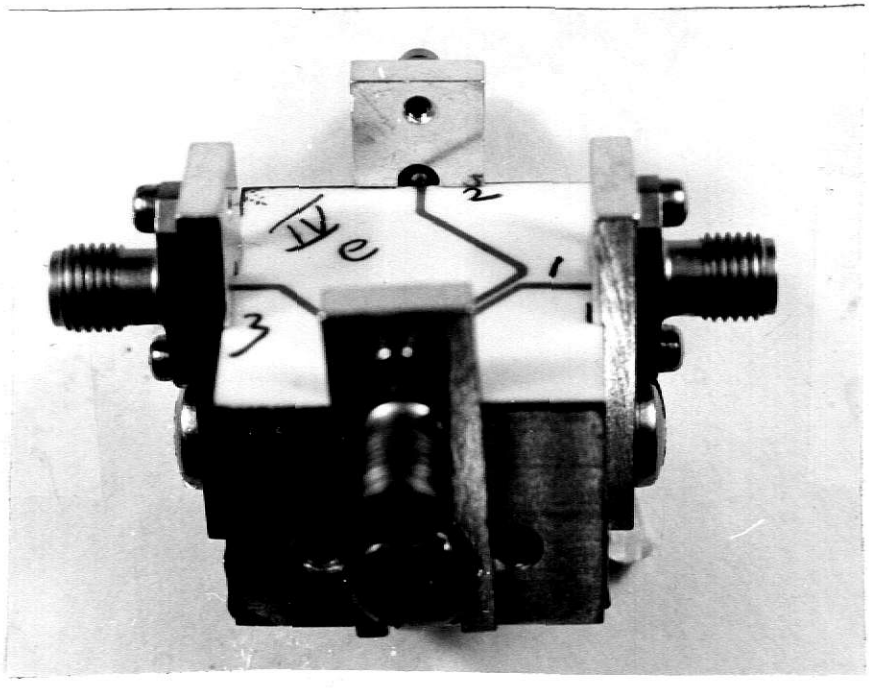

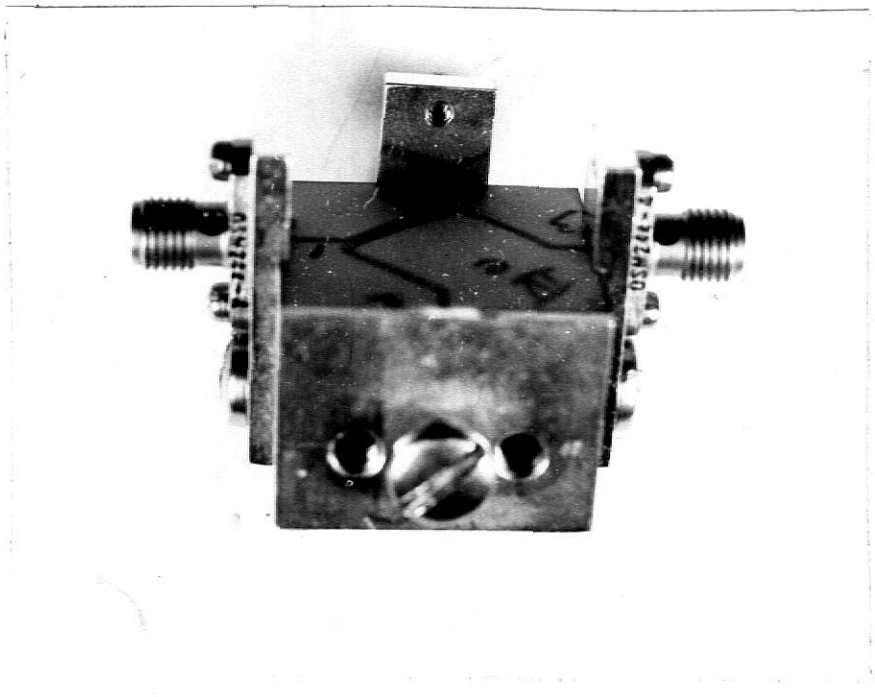

Fig. 13. Microstrip directional coupler and test fixture.

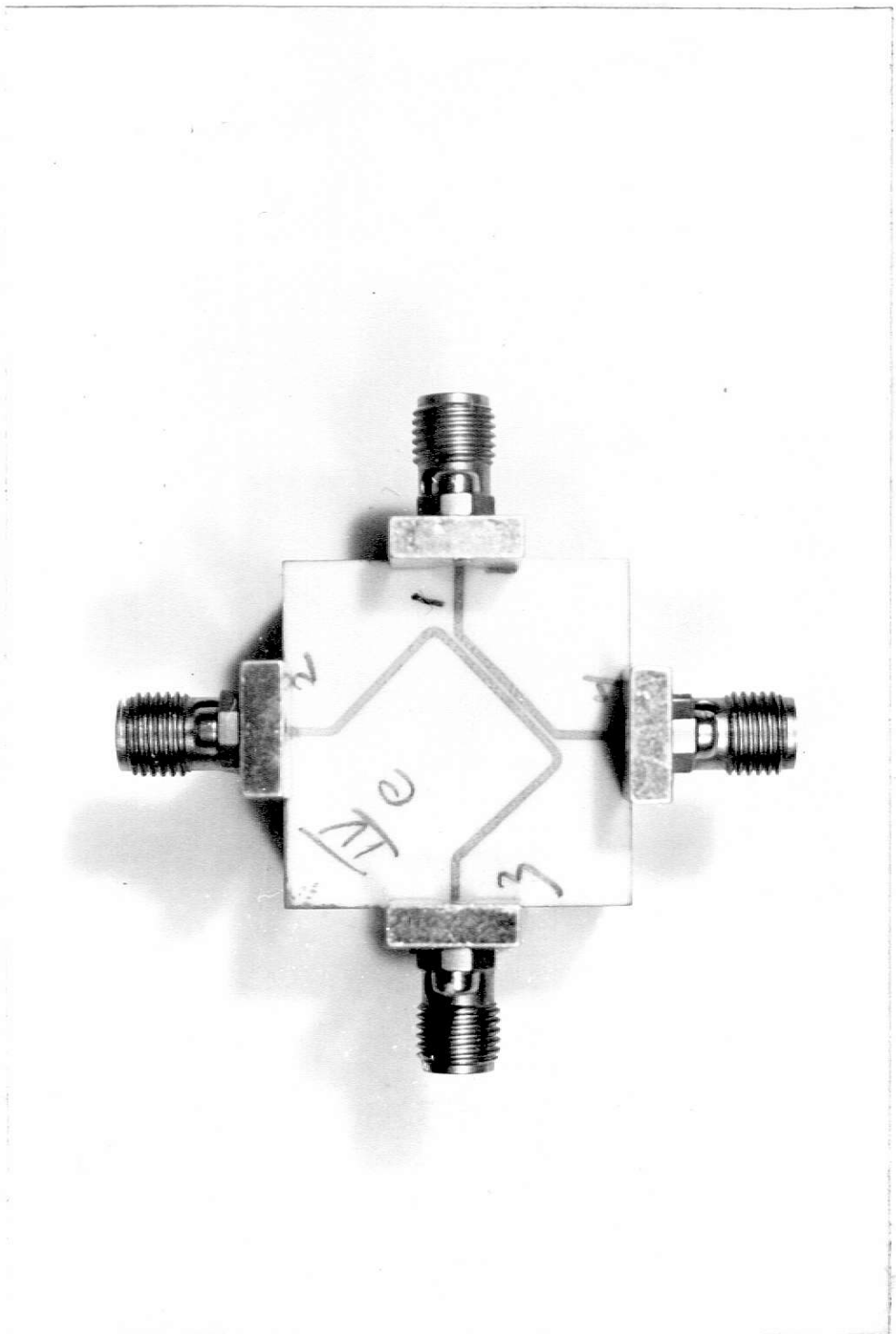

Fig. 13. Continued.

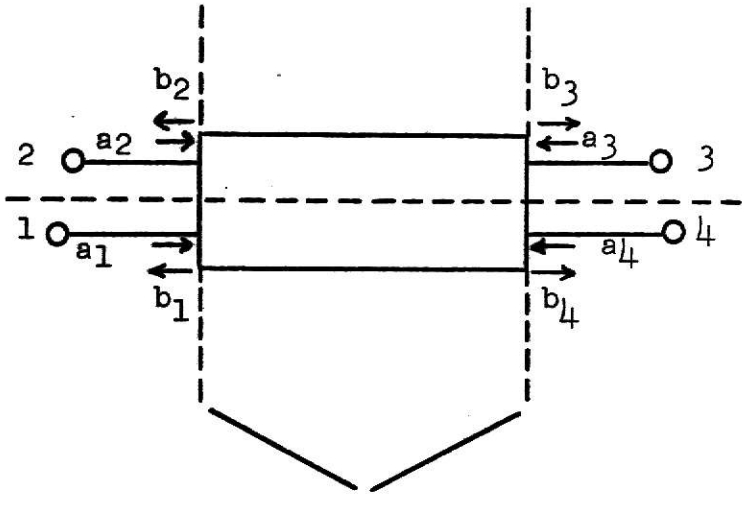

Fig. 14. Scattering parameters associated with a directional coupler.

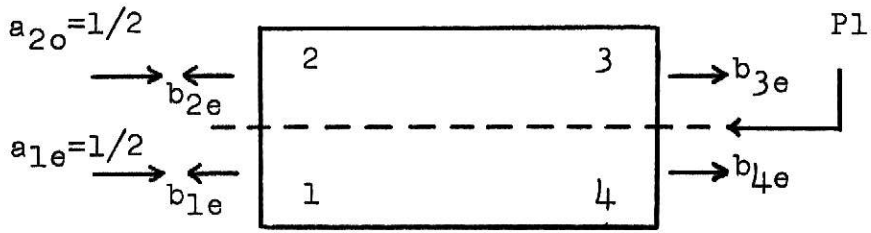

(a) Even mode excitation

$\Gamma_{oe} = b_{1e}/a_{1e} = b_{2e}/a_{2e}$; $T_{oe} = b_{4e}/a_{1e} = b_{3e}/a_{2e}$

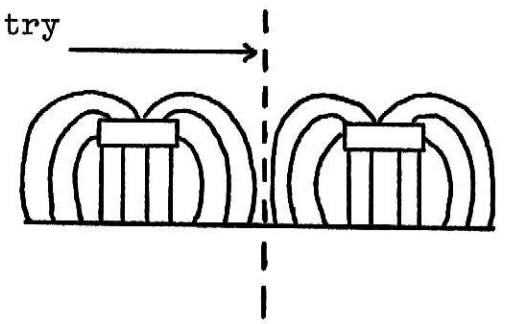

(b) Even mode electric flux configuration

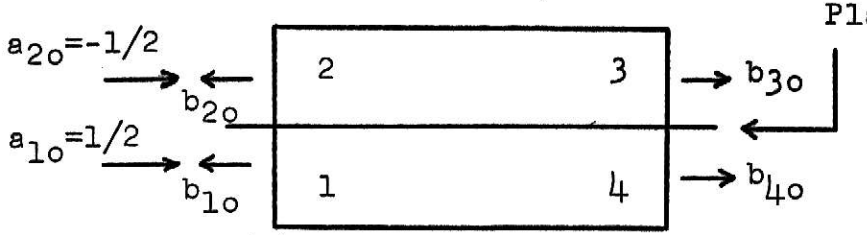

(c) Odd mode excitation

$\Gamma_{oo} = b_{1o}/a_{1o} = b_{2o}/a_{2o}$; $T_{oo} = b_{3o}/a_{2o} = b_{4o}/a_{1o}$

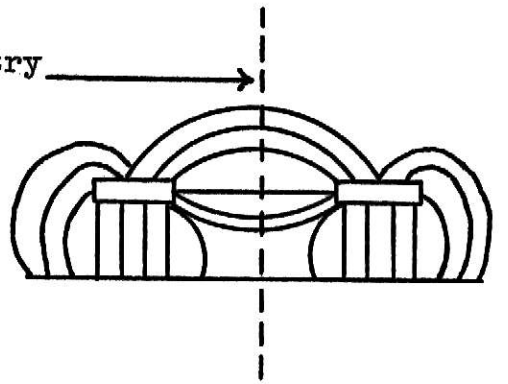

(d) Odd mode electric flux configuration

Fig. 15. Even and odd mode representation.

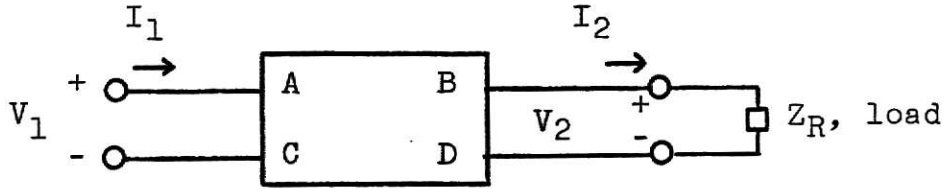

Fig. 16. Cascade matrix circuit representation.

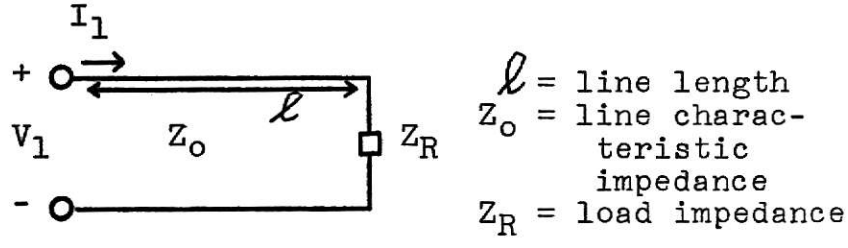

Fig. 17. Transmission line representation.

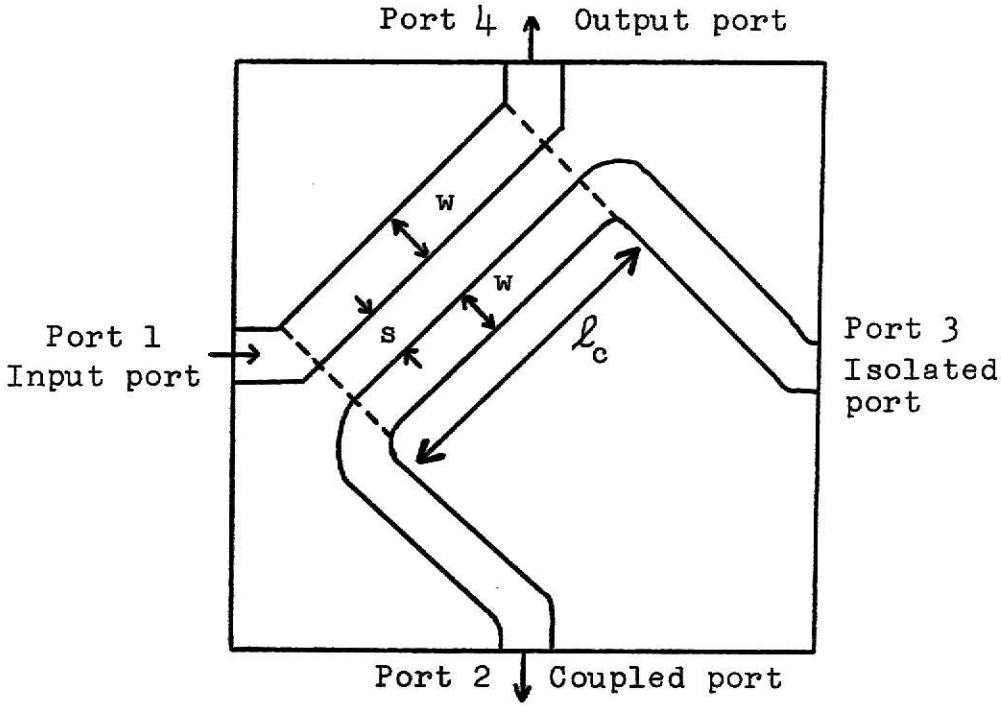

Fig. 18. Microstrip directional coupler.

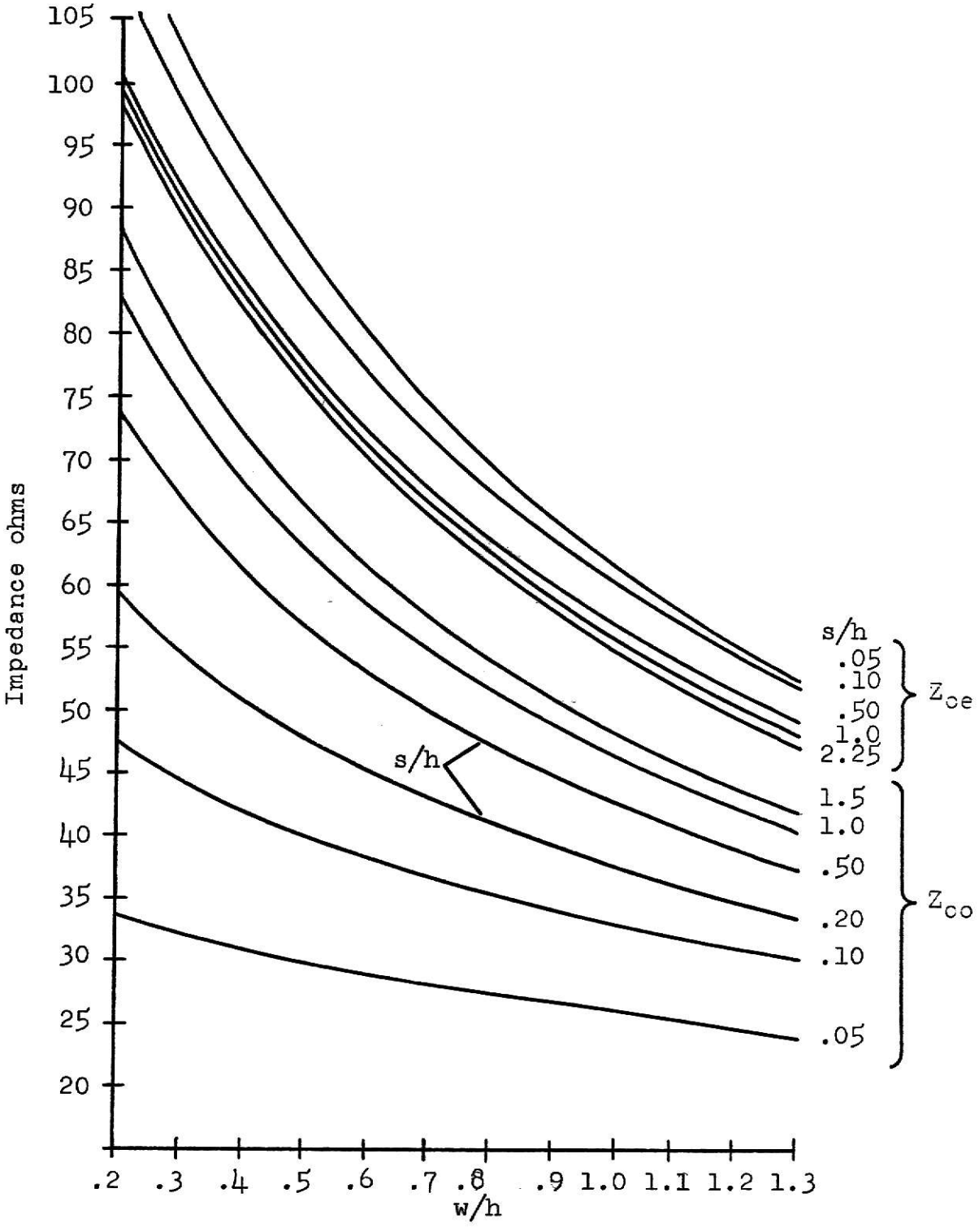

Fig. 19. Design curves for microstrip directional coupler (ϵ_r = 8.9).

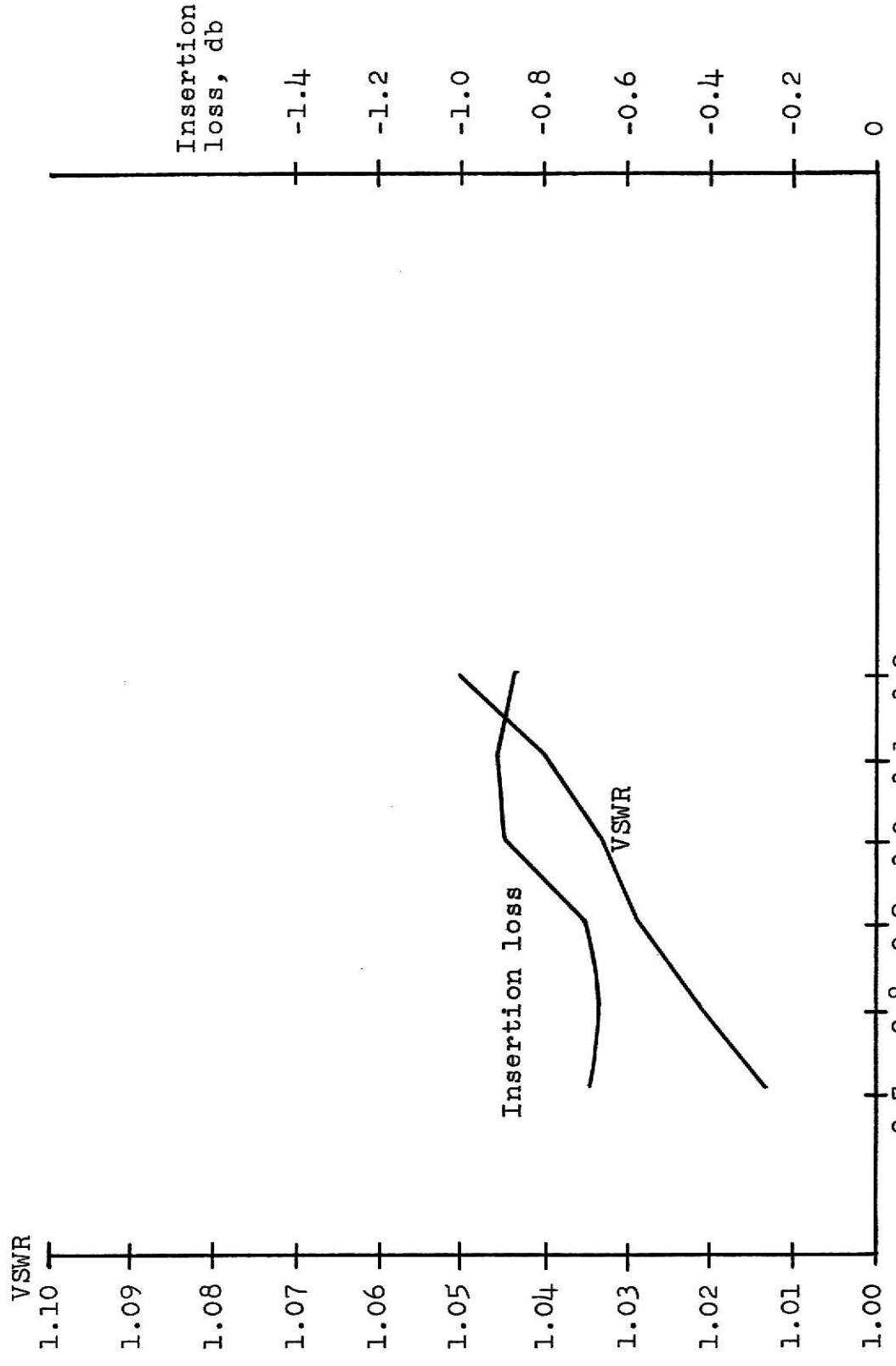

Fig. 20. VSWR insertion loss versus frequency; straight microstrip line (ref. Fig. 2), w/h = 1.0.

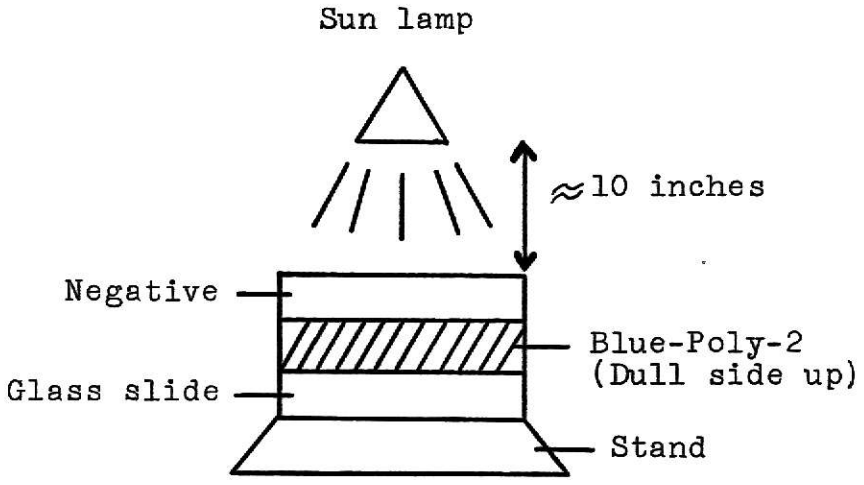

Fig. A-1. Exposure of screen mask.

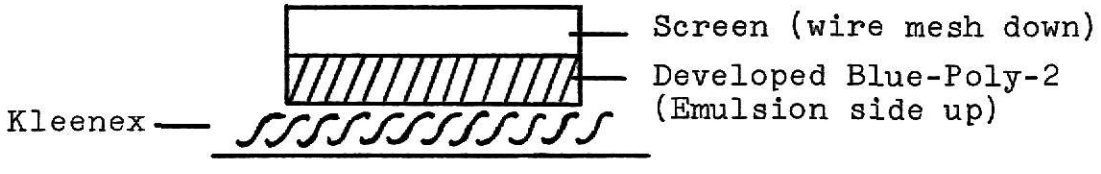

Fig. A-2. Mask to screen transfer.

APPENDIX

A THICK FILM TECHNIQUE AT KANSAS STATE UNIVERSITY

General Discussion

The first step in fabricating an integrated circuit is to prepare the "art work". The "art work" may consist of a rubylith pattern of the circuit or a drawing in black India ink of the circuit. A photograph is taken of the "art work" and the resulting negative is used to make a mask to be deposited on a screen. With the mask formed on the screen, the screen is used for printing the desired circuit pattern on the substrate. The printing is accomplished by forcing a paste through the mask openings with a squeegee. After printing, the substrate is fired in an oven. The detailed steps in fabricating the microwave circuits used in this report are as follows.

I. Forming the Art Work

Use the cutting table to cut a duplicate pattern of the desired circuit. The rubylith was scaled to 5x the desired circuit size. In the photographic process the pattern is reduced to the desired size. It should be noted that the cutting of the rubylith can introduce small errors in width of the circuit conductor paths. These errors will be reduced in the photographic process. For example, the desired path width may be .025 $\pm$.005 inch. Upon scaling (5/1), the dimension of the cut rubylith is .125 $\pm$.025 inch. The error in cutting the rubylith should be no more than $\pm$.001 inch. Thus the error in the photo negative

is reduced to ±.0002 inch. The pattern could be drawn on clear paper with India ink instead of cutting a rubylith pattern.

II. Photographing the Art Work

After the "art work" has been completed, a photographic reduction of the "art work" is needed next. The steps in photographing and developing the negative are:

a. Place the "art work" on an illuminated screen.

b. In a dark room, place the plate film in the camera with the emulsion (dull) side toward the objective. Always make sure that the unused film is placed in its proper container to avoid exposure. The camera settings used were f/11 and time = 1 second; the exposed film is removed from the camera in the presence of red light.

c. The developing procedure is

   1. Pass the exposed film through the developer (1-3 minutes), depending on the strength of the developer;
   2. then through the 'STOP' tray, just dipping the film in and out;
   3. then through the 'FIXER'; leave immersed 6-10 minutes;
   4. wash the film in running cold water for 20 minutes;
   5. hang the negative to dry.

Go through steps 1-2-3 in the prescribed order so as to prevent contamination of the chemicals. Keep the emulsion side up in order to prevent scratching of the exposed surface.

III. Making of the Screen Mask

After the photo negative has dried, the mask for the screen is prepared.

a. Mix the developer according to the instructions recommended by the particular manufacturer. Blue-Poly-2, manufactured by the J. Ulano and Company, Inc., of New York, was the developer used. Keep the mixed developer in a dark room.

b. Arrange the negative, Blue-Poly-2, and sun lamp for exposing the Blue-Poly-2 (Fig. A-1). The exposure time is 8-10 minutes.

c. After exposure, the Blue-Poly-2 is placed in its developer for one and one-half minutes with the film (dull) side up to avoid scratching.

d. Rinse the developed Blue-Poly-2 in running water (92-96° F) until the design is clear. The water temperature is fairly critical and must be maintained between the prescribed limits, and the water pressure must be continually monitored to prevent damage to the Blue-Poly-2.

IV. Screen Preparation

This is the final step in the fabrication process prior to printing the substrate.

a. Place the cleaned, developed Blue-Poly-2 mask on the screen, emulsion (shiny) side up as shown in Fig. A-2.

b. Very gently tap the Blue-Poly-2 through the screen with Kleenex to remove any excess moisture, taking extreme care not to disturb the circuit pattern.

c. Place a small weight (evenly distributed) on the frame of the screen.

d. The screen should then be dried. If air dried, allow 24 hours, or a hot air gun can be used (after two hours of air drying) if the screen is not allowed to become too hot.

e. After sufficient drying, pull the backing of the mask from the screen.

V. PRINTING THE SUBSTRATE

a. Mount the screen on the printer with the screen parallel with respect to the table that supports the substrate. Adjust the screen height above the table to allow for a proper snap-back of the screen. This height partially determines the thickness of the printed circuit. The table can be moved by rotation and translation so as to align the substrate and screen to prevent misregistration.

b. The cleaned substrate must be secured on the table. This may be accomplished by using Scotch tape, an air vacuum, or an appropriate mount.

c. Paste is placed on the screen in the area of the mask opening and slightly before the point of the initial contact of the squeegee and the screen.

d. The squeegee is moved across the screen. There are certain practices that should be followed. They are: do not reprint a substrate; do not attempt to clean the mask while more printing is to be done; only one passage of the squeegee is suggested so as to help maintain a uniform thickness of the pattern. After printing, remove the substrate carefully so as not to smear the freshly deposited paste. Also, care should be taken not to contaminate the unused thick film paste.

VI. Firing Procedure

This procedure is unique to the particular oven available at Kansas State University. For each particular oven the appropriate process must be determined. The procedure followed here was:

a. Place the printed substrates on glass boats and thence into the oven. The oven has a temperature gradient with a maximum at the center.

b. The glass boats are moved gradually from the edge of the oven to the middle and back. That is, two minutes at the edge, three minutes half way in, and fifteen minutes at the center. The reverse timing procedure is used in removing the substrate. The temperature at the center of the oven was 760° F. After removal of the substrates and cooling, the microstrip circuit is ready for use.

This concludes the description of the thick film fabrication process that was employed.

THE DESIGN, FABRICATION AND TESTING OF PASSIVE MICROSTRIP CIRCUITS

by

WILLIAM ALLEN ROSENKRANZ

B.S.E.E., Kansas State University, 1967
B.S., Math., Kansas State University, 1968

AN ABSTRACT OF A MASTER'S REPORT

submitted in partial fulfillment of the

requirements for the degree

MASTER OF SCIENCE

Department of Electrical Engineering

KANSAS STATE UNIVERSITY
Manhattan, Kansas

1972

The objective of this report is to establish the design criteria necessary for the fabrication of microwave microstrip transmission circuits by means of thick film techniques. In the principal application, these techniques were used to build a passive microwave device, a directional coupler.

The first section of this report describes the microstrip line and its characteristic properties. Explicit design curves and equations relating the microstrip line geometry to characteristic impedance are given. Also included are a definite set of guidelines in the use of these equations and graphs for wide, narrow, and intermediate width lines. Consideration is also given to the microstrip line enclosed in a metallic box. Lastly, this section discusses and gives curves for the effective wavelength, effective dielectric constant and filling fraction, and losses for the open microstrip line.

The second section considers the overall design considerations of a thick film microstrip line. Included here is a discussion of the supporting dielectric substrate and its effect in the design and fabrication procedure. Also discussed are thickness and width tolerances in the microstrip center conductor, coupling to the microstrip line, and bends in the microstrip transmission line. This section ends with a description of a thick film fabrication procedure.

The third section demonstrates the use of the microstrip transmission line as a basic building block in fabricating a directional coupler. Included is a scattering matrix and

normal mode analysis of a microstrip directional coupler. A microstrip directional coupler design procedure concludes this section.

The last section gives the design values and test results for microstrip lines of various widths, microstrip lines with bends, and microstrip directional couplers that were fabricated by a thick film procedure at Kansas State University. The test results assure adequate confidence in the design procedure used for the various microstrip circuits. This section concludes with a well defined set of precautions to be observed when employing a thick film procedure to fabricate microwave transmission lines.